M.Tech Microwave and Optical Communication

Pradyut Mohapatra

2022

BIOMEDICAL ANTENNAS AND THEIR APPLICATIONS

A DISSERTATION

SUBMITTED IN PARTIAL FULFILLMENT OF THE REQUIREMENTS FOR THE AWARD OF THE DEGREE

OF

MASTER OF TECHNOLOGY
IN
MICROWAVE AND OPTICAL COMMUNICATION

Submitted by:

PRADYUT MOHAPATRA

2K20/MOC/05

Under the supervision of

ASST. PROF. SUMIT KUMAR KHANDELWAL

DEPARTMENT OF ELECTRONICS AND COMMUNICATION ENGINEERING

DELHI TECHNOLOGICAL UNIVERSITY
(Formerly Delhi College of Engineering)
Bawana Road, Delhi-110042

MAY, 2022

BIOMEDICAL ANTENNAS AND THEIR APPLICATIONS

A DISSERTATION

SUBMITTED IN PARTIAL FULFILLMENT OF THE REQUIREMENTS FOR THE AWARD OF THE DEGREE

OF

MASTER OF TECHNOLOGY
IN
MICROWAVE AND OPTICAL COMMUNICATION

Submitted by:

PRADYUT MOHAPATRA

2K20/MOC/05

Under the supervision of

ASST. PROF. SUMIT KUMAR KHANDELWAL

DEPARTMENT OF ELECTRONICS AND COMMUNICATION ENGINEERING

DELHI TECHNOLOGICAL UNIVERSITY
(Formerly Delhi College of Engineering)
Bawana Road, Delhi-110042

MAY, 2022

DELHI TECHNOLOGICAL UNIVERSITY
(Formerly Delhi College of Engineering)
Bawana Road, Delhi-110042

CANDIDATE'S DECLARATION

I, Pradyut Mohapatra (2K20/MOC/05) student of M. Tech (Microwave and Optical Communication Engineering), hereby declare that the Major Project-II dissertation titled "**Biomedical Antennas and their Applications**" which is submitted by me to the Department of Electronics and Communication Engineering, Delhi Technological University, Delhi in partial fulfillment of the requirement for the award of the degree of Master of Technology is original and not copied from any source without proper citation. This work has not previously formed the basis for the award of any Degree, Diploma Associateship, Fellowship, or other similar title or recognition.

Pradyut Mohapatra

Place: Delhi **PRADYUT MOHAPATRA**

Date: 30/05/2022

DEPARTMENT OF ELECTRONICS AND COMMUNICATION ENGINEERING

DELHI TECHNOLOGICAL UNIVERSITY
(Formerly Delhi College of Engineering)
Bawana Road, Delhi-110042

CERTIFICATE

I hereby certify that the Major Project-II dissertation titled "**Biomedical Antennas and their Applications**" which is submitted by Pradyut Mohapatra (2K20/MOC/05) in the Department of Electronics and Communication Engineering, Delhi Technological University, Delhi in partial fulfillment of the requirement for the award of the degree of Master of Technology is a record of project work carried out by the student under my supervision. To the best of my knowledge this work has not been submitted in part or full for any Degree or Diploma to this University or elsewhere.

Place: Delhi

Date: 30/05/2022

ASST. PROF. SUMIT KUMAR KHANDELWAL

SUPERVISOR

ACKNOWLEDGEMENT

The success and outcome of this project required a lot of guidance and assistance from many people, and I am extremely fortunate to get this all along with the completion of my project work. Whatever I have done is only due to such guidance and assistance and I would not forget to thank them.

I owe my profound gratitude to my project guide **Mr. Sumit Kumar Khandelwal** for giving me the opportunity to do this work. **Mr. Sumit Kumar Khandelwal** toa ok keen interest in my project work and guided me throughout, till the completion of the project work by providing all the necessary information, constant encouragement, sincere criticism, and a sympathetic attitude.

Pradyut Mohapatra

PRADYUT MOHAPATRA

ABSTRACT

Implantable antenna research has gotten a lot of attention recently in the discipline of biomedical engineering. An implantable antenna working in Med-Radio, MICS, WMTS, and ISM bands for biotelemetry applications is presented in this report. The antenna of dimensions 20 x 30 x 1.6 mm^3 has a rectangular C-shaped radiator patch, and an inverted rectangular C-shaped ground plane and CPW feeding is provided. The antenna is placed inside a 70 x 70 x 70 mm^3 container filled with pork tissue for simulation of the real body environment. Here two pairs of substrate-superstrate are considered; the first pair is FR4 epoxy-Rogers RO3010 while the second pair is polyamide-alumina ceramic. At 865 MHz, a maximum SAR value of 1.5948 W/Kg is obtained, for a power input of 22.2 mW, for the former pair while for the latter peak SAR value of 1.5915 W/Kg is observed at a power input of 23 mW and these values are considered safe in accordance with the IEEE standard safety guidelines. The antenna exhibits wideband nature for both the pairs and peak gains of -6.3 dBi and -6.2 dBi are observed at 865 MHz for the respective substrate-superstrate pairs.

This report also presents two conformal antennas for wireless capsule endoscopic systems for robust biotelemetry communications, one of them covers the 865 MHz band and the other one covers both 865 MHz and 2.4 GHz ISM bands.

Biotelemetry is one of the applications of these bands. Two planar antennas are designed first and then they are conformed around a cylindrical capsule. It is observed that the antennas have wider bandwidth at respective bands. The peak realized gain for both antennas at 865 MHz is -18.1 dBi while the antenna with a bow and arrow shaped radiator has a peak gain of -13.3 dBi at 2.4 GHz. Since the capsule needs to be ingested by the patient for endoscopy, biocompatibility has been ensured. The maximum SAR values are obtained for both the antennas and are considered safe in accordance with the IEEE standard safety guidelines. The recommended antennas' conformal design idea, omnidirectional radiations, and multiband capability with wider bandwidth in the ISM band(s) will improve the scope for capsule endoscopy and would provide valuable contribution in the domain of biotelemetry. The simulation is performed in ANSYS Electronics Desktop simulation software.

CONTENTS

LIST OF FIGURES

LIST OF TABLES

LIST OF ABBREVIATIONS

IMD	Implantable Medical Device
SAR	Specific Absorption Rate
MedRadio	Medical Device Radiocommunications
MICS	Medical Implant Communications Service
WMTS	Wireless Medical Telemetry Service
ISM	Industrial, Scientific, and Medical
PIFA	Planar Inverted-F antenna
AEDT	Ansys Electronics Desktop
WCE	Wireless Capsule Endoscopy
GI	gastrointestinal

CHAPTER 1

INTRODUCTION

IMDs are medical devices that are surgically implanted into a patient's body and are used for a range of monitoring, diagnostic, and therapeutic reasons. IMDs include cardiac pacemakers, implantable cardiac defibrillators, medication infusion pumps, glucose monitors, insulin pumps, neurostimulators, and others. Biocompatibility refers to the property of materials that do not cause harmful injuries or reactions in humans.

Capsule endoscopy is a procedure that includes examining GI tract of a patient with a small wireless camera. As the camera, which is housed within a pill, travels through one's digestive tract, it captures multiple images. Capsule endoscopy, as opposed to traditional wired cable-connected endoscopies, provides better diagnosis and treatment with less pain and discomfort for patients [1].

1.1 IMPLANTABLE ANTENNA

As the healthcare industry has advanced, biomedical telemetry has attracted a lot of attention. IMDs serve a critical role in healthcare monitoring via wireless telemetry, by allowing communication with an external device and transferring data from sensors

located within the human body. These devices enable the real-time communication of a patient's physiological data to an external unit, such as glucose level, temperature, cardiac pulse, and so on. Patients' vital signs can now be monitored remotely, without the need for typical hospital check-ups or follow-up routine check-ups, owing to this technology. Implantable and wearable biotelemetry devices are two types of biotelemetry devices. The implantable antenna has several drawbacks. To have a robust and continuous performance, various variables such as low power consumption, miniaturisation, patient safety, lower operating frequency band, and multiband or wideband operation must be considered for implantable sensors. The characteristic that impacts the implant's overall performance is the selection of antenna structure in the design of implantable sensor, which is a challenging task.

IMDs must be able to wirelessly share data with outside monitoring/control equipment to be genuinely effective in ensuring patient comfort. IMDs have recently shifted their focus to antenna-enabled medical telemetry. Implantable antennas are required for wireless data transfer from implants to the outside world. Smart implants can track and diagnose medical conditions. Implanting an antenna within the human body is a difficult task.

The implanted sensory units are inserted inside the human body and monitor heart rate, respiratory rate, blood pressure, temperature etc. and transmit the data, which they have collected, to an external unit. Implantable antennas usually operate at MedRadio (401-406 MHz), MICS (402-405 MHz), WMTS (1.427-1.432 GHz), and/or ISM (433-434 MHz,865-867 MHz and 2.4-2.48 GHz) bands [2]. To ensure biocompatibility of implantable antenna, biocompatible encapsulation is used. The materials used for this purpose are polyetheretherketone (PEEK), Silastic MDX-4210 Elastomer and Zirconia [3]. Due to its electromagnetic characteristics, zirconia (ε_r = 29) is a preferable alternative for bioencapsulation. It has a very low loss tangent and a very high permittivity value, which significantly reduces the loss of power by

confining the near field of the antenna inside the capsulation. The amount of electromagnetic radiation absorbed by the human body is described as the SAR. According to IEEE C95.1-1999 rules, the average SAR for 1 g of human tissue should be less than 1.6 W/kg.

1.2 CAPSULE ENDOSCOPY

Capsule endoscopy is an outpatient procedure that obtains pictures of your digestive tract. In this technique, a pill-sized wireless camera is ingested by the patient. The camera takes many images as it goes through one's digestive tract. The doctor can view the patient's small intestine without the need of performing an operation [4]. Capsule endoscopy can detect and identify anatomical changes in the small intestine like ulcers, Crohn's disease, Celiac disease, Gastrointestinal cancer, and other gastrointestinal illnesses.

Capsule endoscopy has several advantages over conventional endoscopic techniques. This procedure can investigate the small intestine, which can be difficult to reach during an upper endoscopy or colonoscopy. In classic endoscopic treatments, a flexible tube with a video camera passes through one's digestive tract which can be painful. In contrast, capsule endoscopy is as simple as swallowing a tablet. The disposable capsule travels through the rest of the gastrointestinal tract before being excreted from the body naturally and painlessly. It can also identify intestinal issues that are not obvious on imaging tests such as x-rays or CT scans. Capsule endoscopy provides the added benefit of requiring minimal preparation and no anaesthetic. Usually, capsule endoscopy is a painless and risk-free process. It does, however, have a few flaws. The capsule has a very modest probability of becoming stuck in the patient's small intestine and causing a blockage. Fig 1.1 shows the dimensions of capsule.

Figure 1.1 Dimensions of capsule

Two types of antennas are considered for capsule endoscopy. The antennas installed inside the capsule cavity are embedded antennas. While conformal antennas only use the capsule module's surface, leaving the interior free for other equipment, allowing the capsule's surface area to be used as efficiently as possible. Since there are various ISM bands available, choosing the right operating frequency is critical. The 433 MHz ISM band, for example, has small bandwidth; the 2.4 GHz ISM band, on the other hand, has a larger bandwidth but higher path loss. Wireless systems such as Zigbee and Bluetooth can cause significant obstruction as they operate in the corresponding ISM band [4]. As a result, the 865 MHz ISM band is preferred.

CHAPTER 2

LITERATURE REVIEW

For operating at MedRadio, WMTS, and ISM bands, a unique S-shaped quad-band PIFA antenna is proposed for the purpose of implantable biotelemetry [2]. The suggested antenna has a compact size of 245mm3, consists of three substrates and a superstrate, and made up of three layers: S-shaped radiator in one layer and two twin spiral radiators in other layers. The antenna has bandwidths of 150MHz for the MedRadio and 433 MHz ISM band, 52MHz for the WMTS band, and 102MHz for the 2.4 GHz ISM band. Peak gain for 401 MHz is 22 dBi, 433 MHz is 23 dBi, 1.427 GHz is 17 dBi, and 2.4GHz is 16 dBi. The suggested antenna has sufficient properties to support implantable body area networks (BAN) for biotelemetry applications and can entirely cover the major bands for BAN below 3 GHz.

In paper [5], an implantable circular polarized (CP) antenna has been illustrated which operates in the 2.40 GHz ISM band. To successfully minimise the antenna size and expand its CP bandwidth, the authors have used a notched ring slot and shorting pin methodology. The size of the antenna is 9.8 x 9.8 x 1.27 mm^3 where $0.0784\lambda_0$ = 9.8mm and $0.0102\lambda_0$ = 1.27mm. Also, the impedance bandwidth and axial ratio bandwidth are also considerably enhanced. The percentage bandwidth based on simulation is 21.5% with peak gain of -33 dBi. The antenna is also resistant to a variety

of biocompatible coating thicknesses. The impact of various body phantoms is explored to assess the suggested antenna's sensitivity.

In [6], a compact dual-antenna setup with improved isolation is investigated for 2.40 GHz ISM band biotelemetry applications. As a primary antenna element, a miniaturised antenna based on a resonator (T-shaped) and a shorting through is designed. Then, a small dual antenna system with a size of 0.084 λ_0 x 0.168 λ_0 x 0.01 λ_0 is modeled. After that, using the neutralisation line between the two radiating elements and the DGS, the antenna system's inter-element coupling is greatly reduced to -37 dB. Furthermore, the suggested antenna's Specific Absorption Rate (SAR) is assessed to ensure that it meets the health safety standards. A wireless link budget analysis is conducted that meets the requirements for a high-speed biotelemetry application satisfactorily. The proposed antenna has fractional bandwidth of 8.5% and gain of -28.3 dBi.

Two spiral coupled resonators are employed to obtain broader bandwidth at lower bands in an implantable antenna to operate in MICS and 2.4 GHz ISM bands [7]. This dual-band antenna has dimensions of 16.5 x 16.5 x 2.54 mm^3 and gain of -30 dBi. The bandwidths obtained from testing are 13% and 4.4% at MICS and ISM bands, respectively, and the simulated bandwidths are 12.6% and 5.7% at MICS and ISM bands, respectively.

To cover the MedRadio band, this research presents an implantable wide-band antenna. This antenna, consisting of a monopole radiator with a ground plane (C-shaped), is proposed in [8]. The coupling between the ground plane and the sigma-shaped radiator enabled an additional resonant mode. To accomplish perfect impedance matching, a CPW feeding line is used. The suggested antenna is small,

measuring only 560 mm^3 in size. The antenna operates in MedRadio band with gain of -27.8 dBi. For maximum input power of 10.1 mW, this antenna has considerably safer SAR values.

A miniaturised antenna for a WCE system resonating at 915 MHz is proposed in paper [4]. Experiments show that the antenna has a wide frequency bandwidth of 300 MHz for a very small size of 7 x 7 mm^2, where 0.021 λ_0 = 7 mm. The antenna is placed on a 675 μm thick double-sided polished high resistive silicon (HRS) substrate (ε_r = 11.9 and tan δ = 0.001). It is installed on a chip-on-board (COB) with a balun and a SMA connector for measuring purposes. For biotelemetry applications, link budget analysis is carried out. The pathloss in the human phantom is less than 52 dB for all capsule configurations, paving the way for enhanced ingestible WCE by allowing higher data rate communication with the receiver placed outside the body, making it a suitable choice for GI tract imaging WCE system. The peak gain at 915 MHz is -35.5 dBi.

Two conformal antennas for wireless telemetry [9] have been proposed for the applications of WCE. A helical and a meander line antenna have been simulated, built, and measured in a human body tissue environment. Capsule system dimensions are 30mm x 10mm on the outside, and 8.6mm on the inside. For helical and a meander line antenna, fractional bandwidths of 51.3 percent and 20.8 percent, respectively, were found, with maximum gains of -28.3 dB and -41.3 dB.

A conformal ultrawideband (UWB) meandering loop antenna has been proposed for WCE applications [10]. The antenna has a height of 14 mm and diameter of 10 mm. In planar form, the antenna is 28 mm in length and 14 mm in width. A 254 μm thick polytetrafluoroethylene (PTFE) substrate was used to develop and fabricate

the antenna. The antenna's bandwidth is 164% of the fractional bandwidth, ranging from 200 MHz to 2.05 GHz. It emits omnidirectional radiation with a maximum gain of –31.5 dBi.

A small antenna with WCE that operates in the 433 MHz ISM band is described in the study [11]. A monopole printed on the substrate with a partial ground plane acts as a receiving antenna which is placed on the body of patient, while the in-body transmitting capsule is a UWB loop antenna conformed around it. The in-body antenna is composed of Preperm 255 and is attached to the capsule's exterior wall. The capsule has a wall thickness of 0.5 mm, a radius of 5.5 mm, and a length of 27 mm, respectively. With a max achieved gain of -23 dBi, the fractional bandwidth is found to be 112.5 percent.

A loop antenna with a meander design is proposed for a UWB endoscope system built on the capsule's exterior surface [12]. The interior and exterior radius of the capsule are 5 mm and 5.5 mm, respectively. The proposed antenna is built of a flexible PCB with a 25.4 μm thick polymide layer. Fractional bandwidth of 52% is obtained.

A conformal, implantable and UWB antenna is designed to be used for WCE in this study [13]. The antenna can be attached to the capsule surface to make the most of the space available. The results obtained from simulation show that this antenna performs well with a wider bandwidth of 541 MHz. At 403 MHz, the maximal achieved gain is 31.5 dBi.

2.1 MICROSTRIP PATCH ANTENNA

Microstrip antennas can be printed directly onto a circuit board and so they have become quite popular. Since they can be made conformal for integration into clothing, the patch antenna is highly suited for any wearable application. Microstrip antennas have many operating restrictions, including high quality factor, low power, low efficiency, poor polarisation purity, poor scan performance, spurious feed radiation, and a very small frequency bandwidth (typically smaller) [16].

In the microstripline feeding approach, a conducting strip is attached directly to the edges of the patch, as shown in Fig. 2.1. This feed configuration allows the feed to be engraved on the same substrate as the patch, resulting in a planar structure, because the strip is thinner than the patch. The objective of inset cut is to match the impedance of the feed line to the patch without the use of any further impedance matching components. A patch antenna resonating at 2.4 GHz has been simulated on AEDT software. The antenna with the substrate as FR4 epoxy uses inset feed as shown in Fig. 2.2. From the microstrip patch antenna calculator, length and width of patch must be 28.86 mm and 37.26 mm respectively, while edge impedance is found out to be 243 Ω.

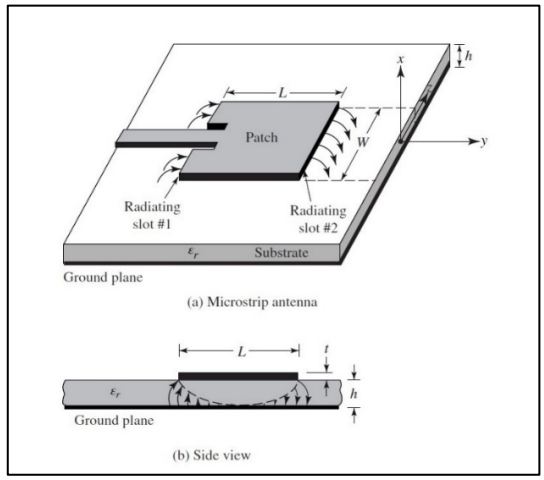

Figure 2.1 Microstrip patch antenna

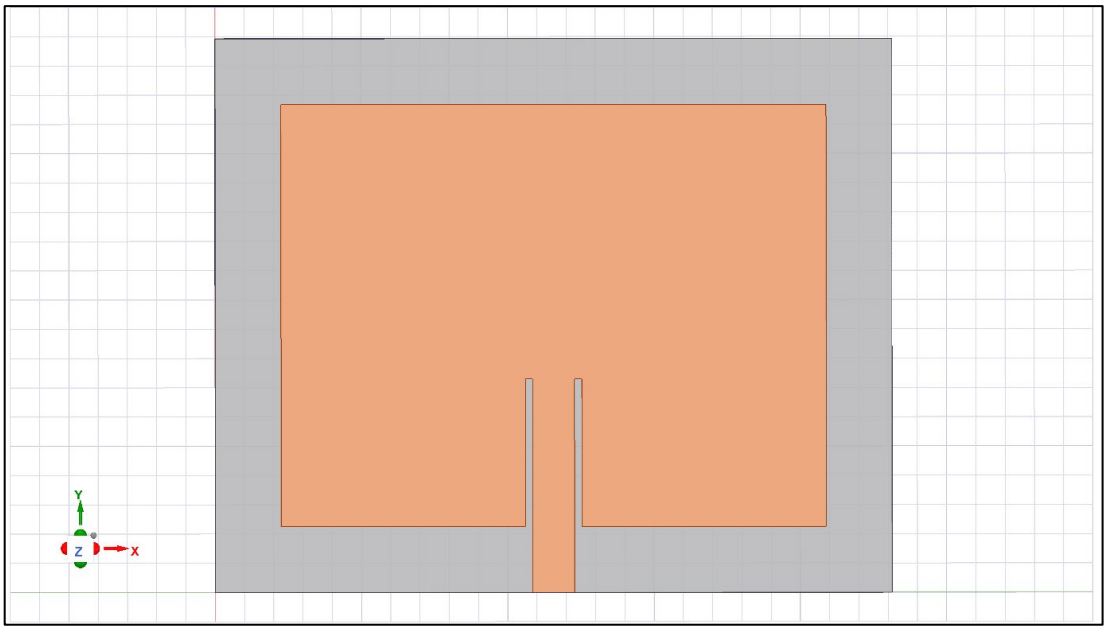

Figure 2.2 Simulation design

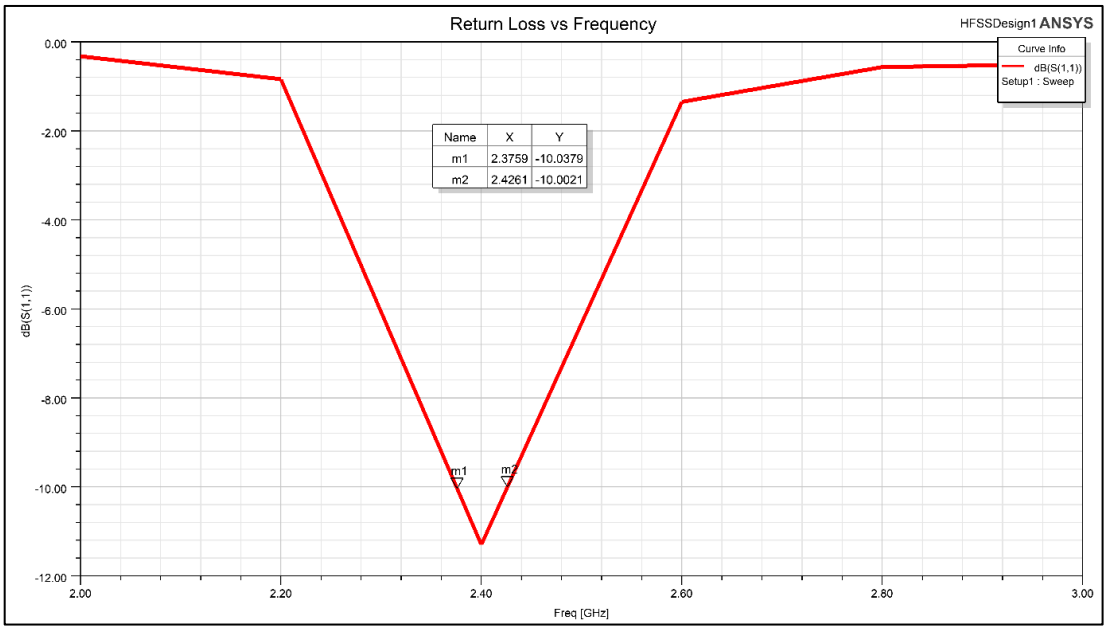

Figure 2.3 Return Loss vs Frequency

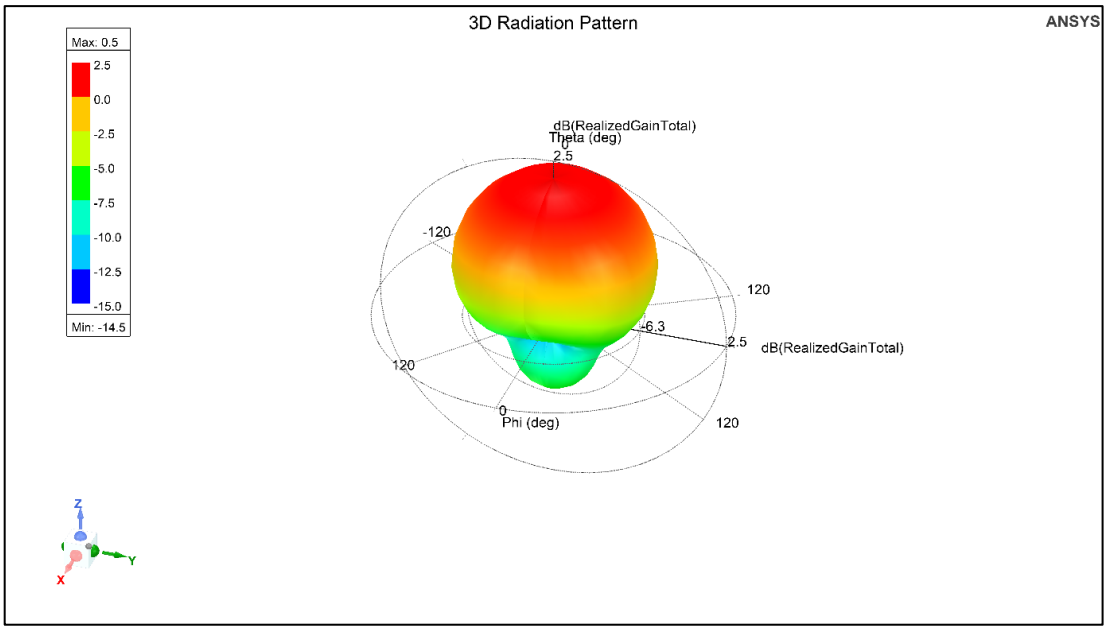

Figure 2.4 3D Radiation Pattern

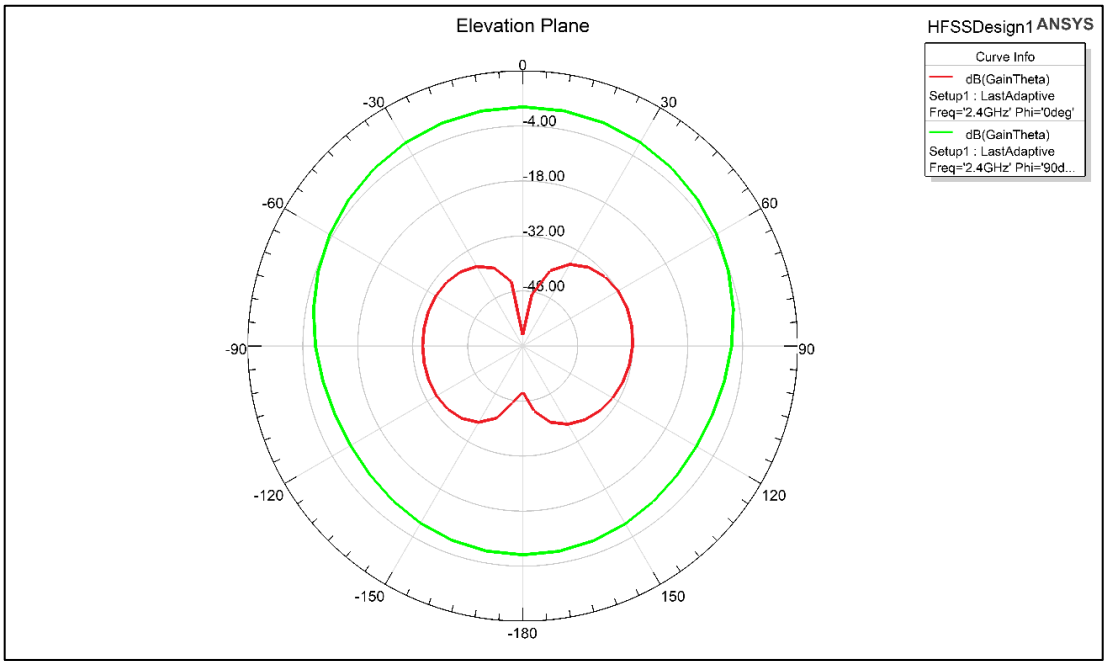

Figure 2.5 Elevation Plane

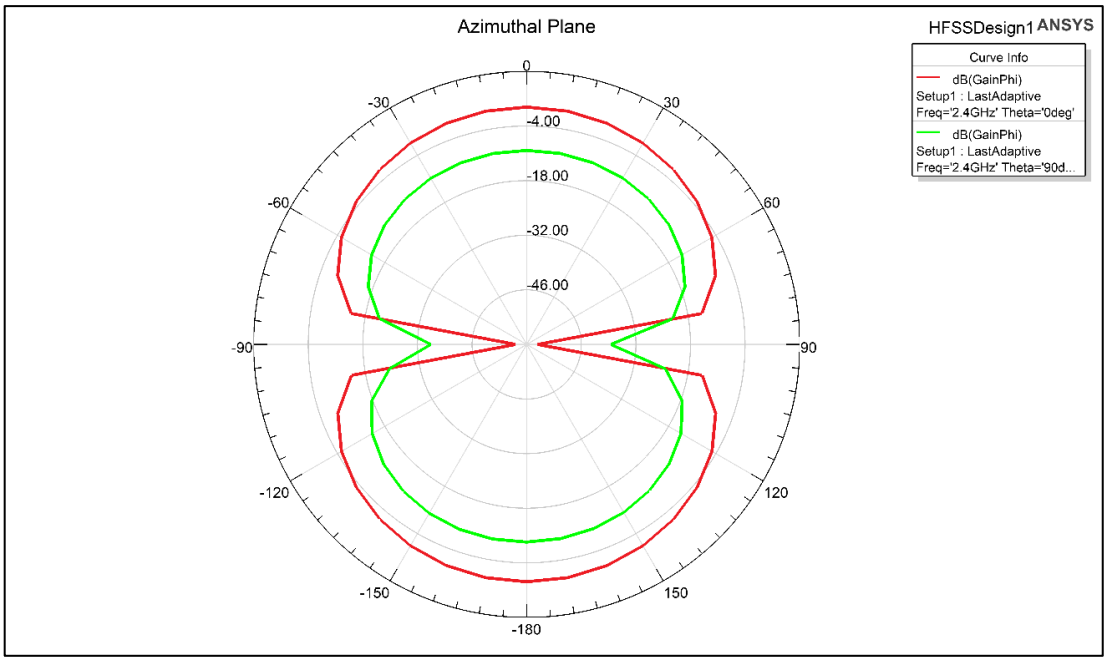

Figure 2.6 Azimuthal Plane

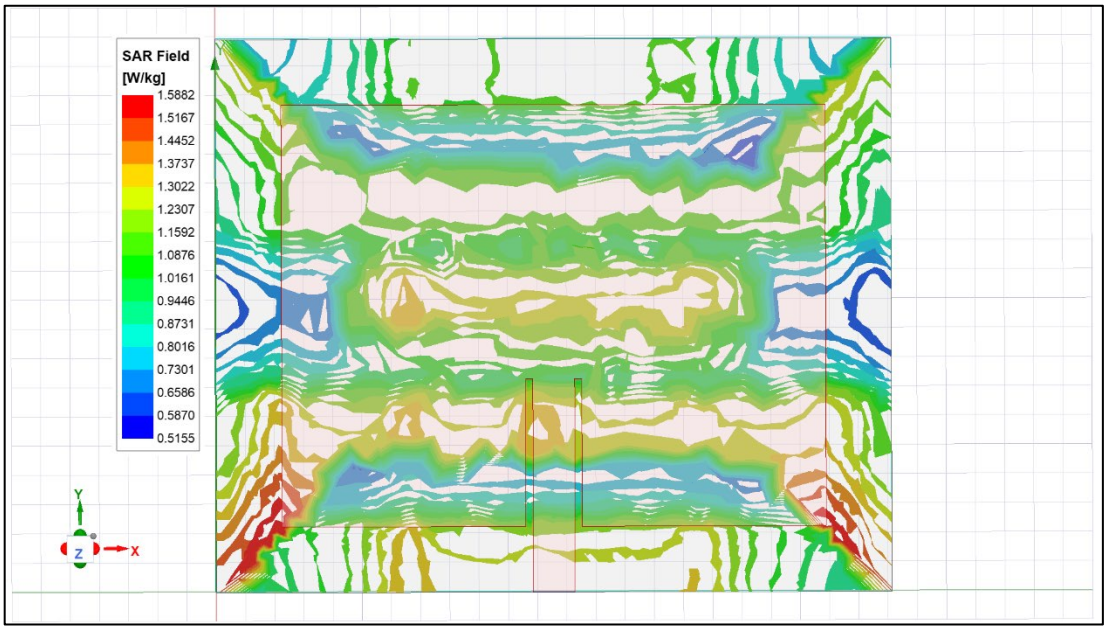

Figure 2.7 SAR field

Impedance bandwidth of 50.2 MHz is observed at the resonant frequency. It is observed that the maximal gain of the antenna is 0.5 dB. 2D Radiation patterns are observed in the fig. 2.5 and fig. 2.6. It can be concluded that for the patch antenna to operate at lower frequencies, its size must be larger than what is now but for

biomedical uses the size of antenna must be smaller. Also, it is observed that the antenna has narrow bandwidth and low gain, which is not suitable for biomedical purposes.

2.2 OBJECTIVES

An innovative design to achieve the wideband nature for the implantable antenna to operate in Med-Radio, WMTS, MICS, and ISM bands has been presented. A rectangular C-shaped radiator and an inverted rectangular C-shaped ground plane have been considered for the antenna design. FR4 epoxy ($\varepsilon_r = 4.4$) and Roger's RO3010 ($\varepsilon_r = 10.2$) are considered for the substrate and superstrate of this antenna, respectively. To ensure biocompatibility, Zirconia coating can be used for bio-encapsulation. Further, polyamide ($\varepsilon_r = 4.3$) and alumina ceramic ($\varepsilon_r = 9.8$) are used as substrate and superstrate respectively without altering the structure of the antenna. Both the antennas are modeled and simulated on AEDT software. Parameters of the antenna design and experimental results obtained from simulation are also discussed.

Also, in this project, conformal antennas are discussed for WCE. Two cases are considered for conformal antenna. In case 1, the antenna radiator is a simple T-shaped structure which operates only at the 865 MHz band. For case 2, the structure of the radiator is modified, and the antenna now resonates in the both 865 MHz and 2.4 GHz bands. Wider bandwidth is observed for both the cases. Also, the SAR value observed is considered safe. The planar antennas are wound around the cylindrical capsule structure which is placed in a box that depicts the human body environment. To ensure biocompatibility, Teflon substrate ($\varepsilon_r = 2.1$) and ULTEM capsule have been considered. The simulated results are observed with the help of AEDT.

CHAPTER 3

BIOMEDICAL IMPLANTABLE ANTENNA

3.1 IMPLANTABLE ANTENNA

The proposed antenna operates at all the biomedical frequency bands i.e., MedRadio, MICS, WMTS and ISM bands. With the help of AEDT simulation software, an implantable antenna is designed which operates at the frequency bands mentioned above. For the simulation setup, multiple frequencies- 401 MHz, 433 MHz, 865 MHz, 1.427 GHz and 2.4 GHz are selected. The antenna comprises of a rectangular C-shaped radiator patch, and an inverted rectangular C-shaped ground plane in a single layer as shown in fig. 3.1 as well as fig. 3.3. A Roger's RO3010 (ε_r = 10.2) superstrate and an FR4 epoxy (ε_r = 4.4) substrate are used as shown in fig. 3.2. In order to attain perfect impedance matching, CPW technique is used. In this paper, the 20 × 30 × 1.6 mm^3 antenna is positioned at the center of a 70 × 70 × 70 mm^3 container which is filled up with pork tissue to present an ideal body environment. Table I displays the measurements of the proposed antenna structure.

Table I. Dimensions of antenna

DIMENSIONS	VALUE (mm)
a	20
b	30
c	9.45
d	0.75
e	9.2
f	7.5
g	20
h	2
i	2
j	7
s	0.8
t	8.25

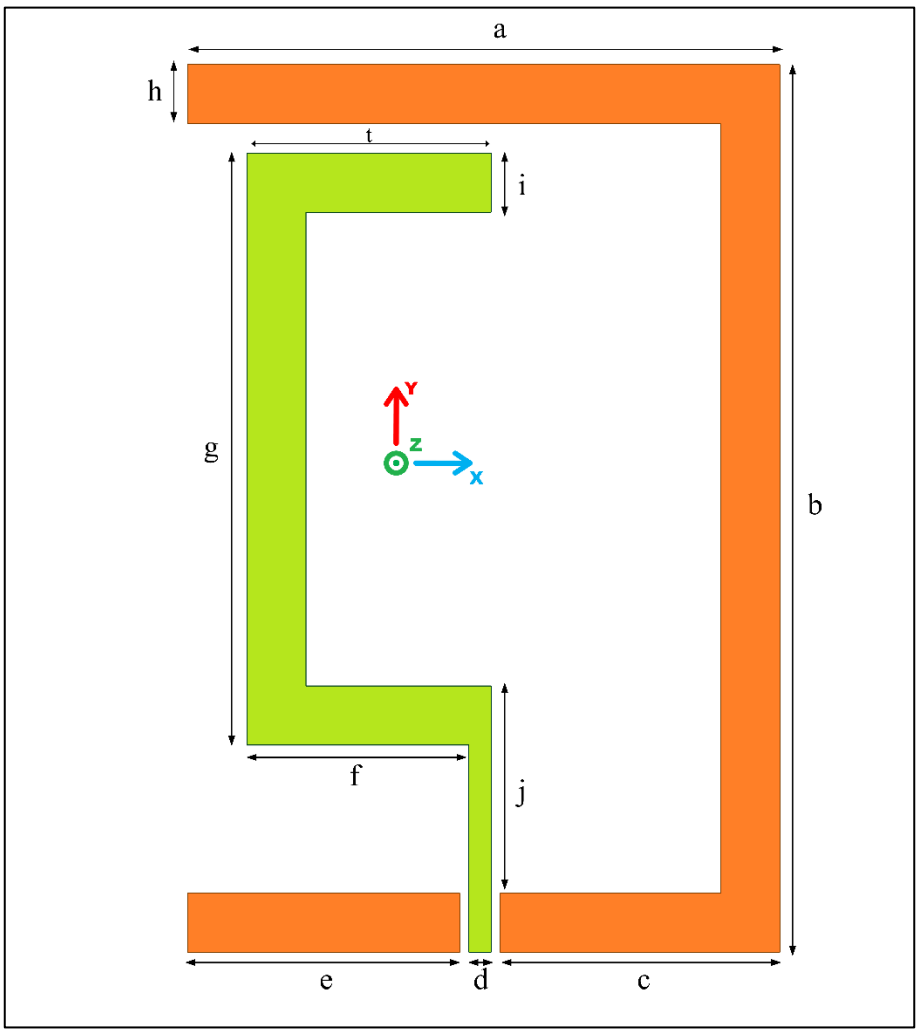

Figure 3.1 Top view of antenna

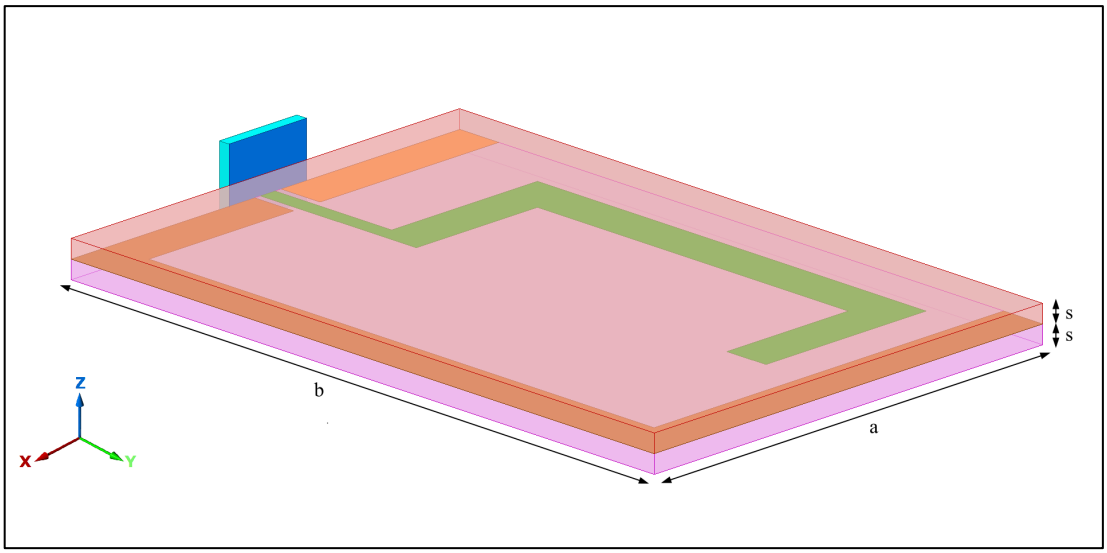

Figure 3.2 Dimetric view of antenna

3.1.1 Simulation and Results

Gain, radiation pattern, efficiency, and SAR are all factors to be addressed while developing an implantable antenna. The designed antenna is simulated in ANSYS's simulation software and the results obtained are plotted. It is observed from fig. 3.4 that the antenna behaves as a wideband antenna as it resonates from 360.4 MHz to 3 GHz and beyond, so it covers MICS band, MedRadio band, 433MHz ISM band, 865 MHz band, WMTS band, and 2.4 GHz ISM band. Radiation efficiency of the antenna increases with frequency (see fig. 3.5).

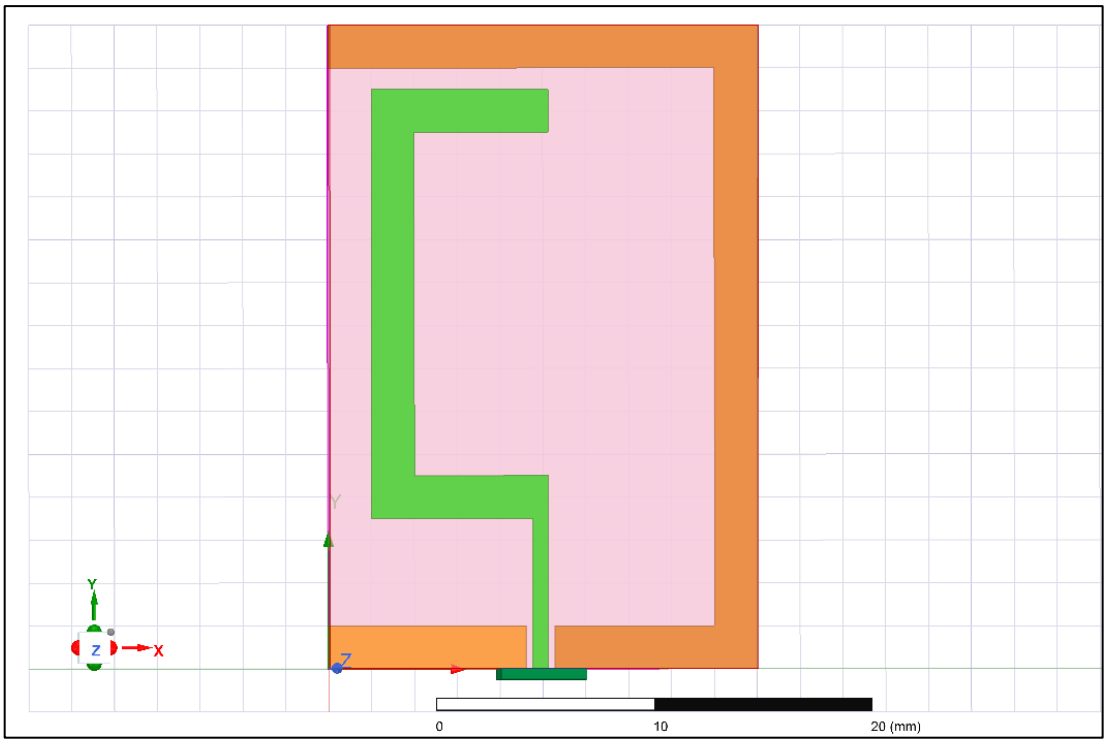

Figure 3.3 Simulation design

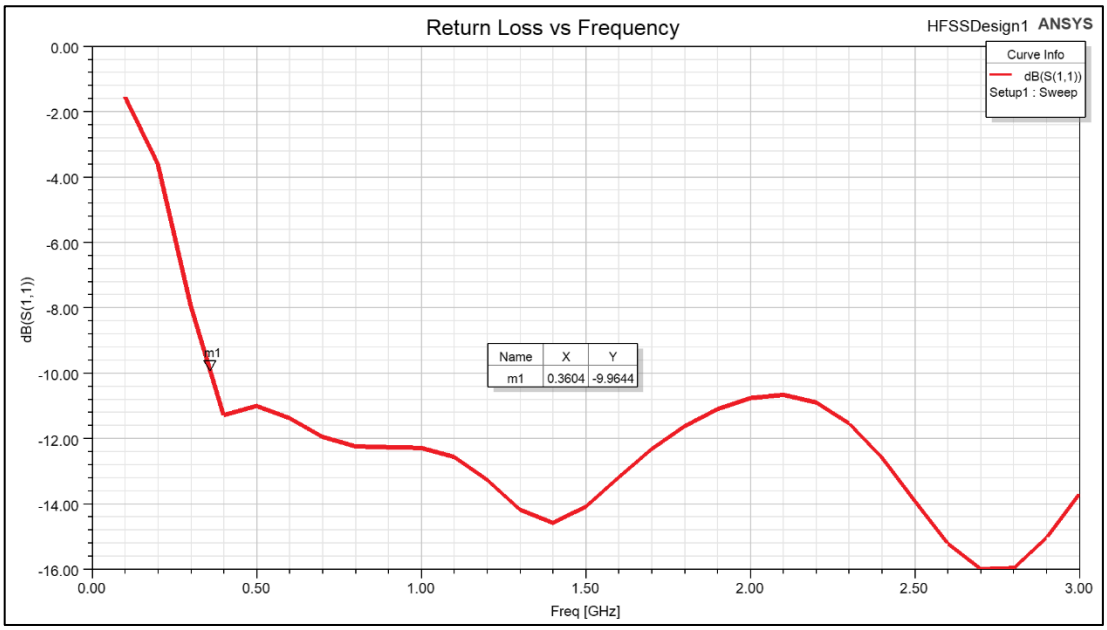

Figure 3.4 Return loss vs Frequency

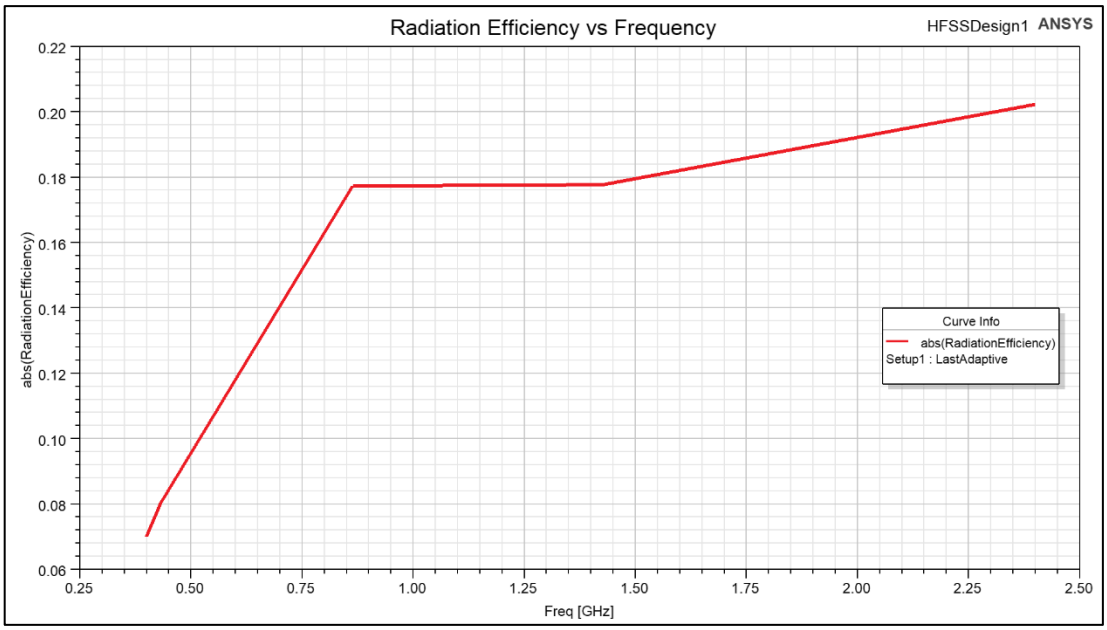

Figure 3.5 Radiation Efficiency vs Frequency

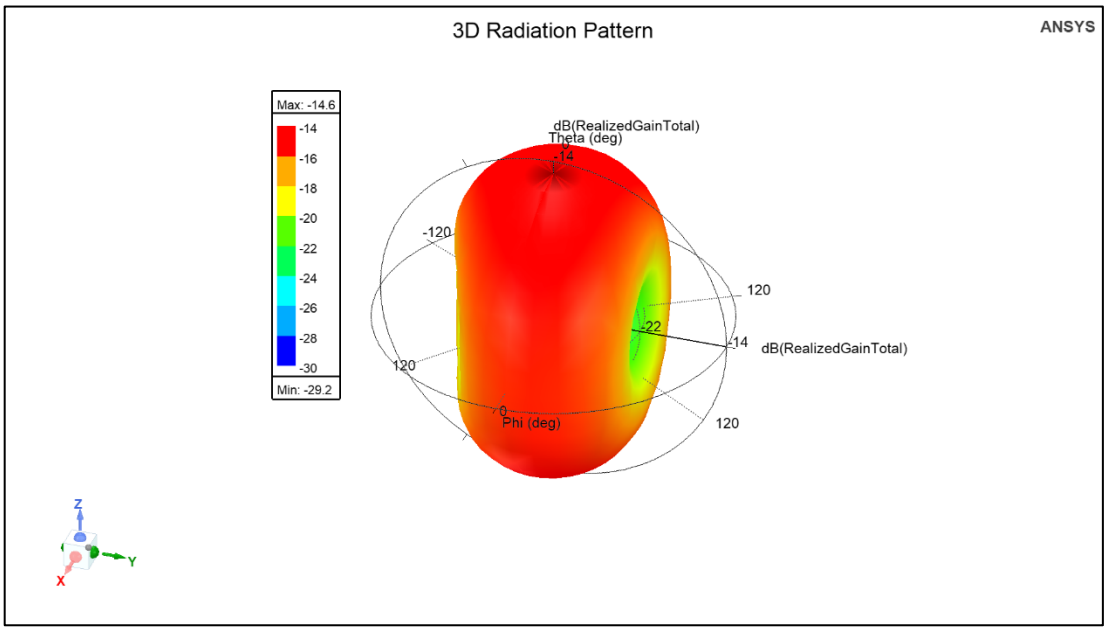

Figure 3.6 3D Radiation Pattern

At 401 MHz, it is evident that peak gain is -14.6 dBi, which is better in comparison to other antennas discussed in section 1. 2D radiation patterns are observed. For input power of 9.85 mW, SAR value is 1.597 W/kg which is considered safe for 1g of human tissue (refer fig. 3.6 – 3.9).

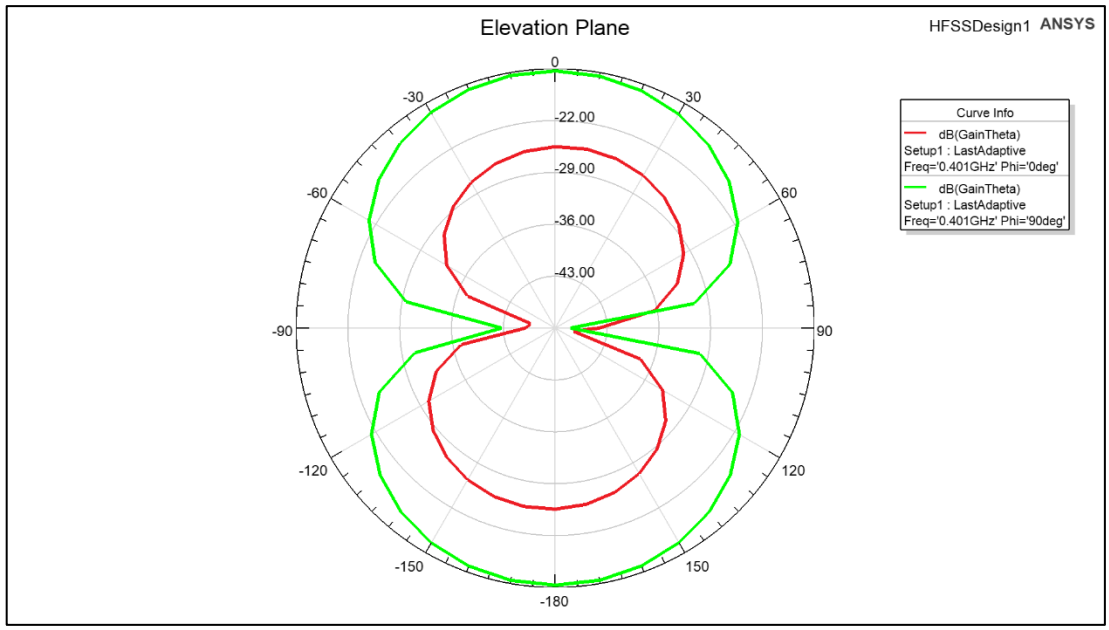

Figure 3.7 Elevation Plane

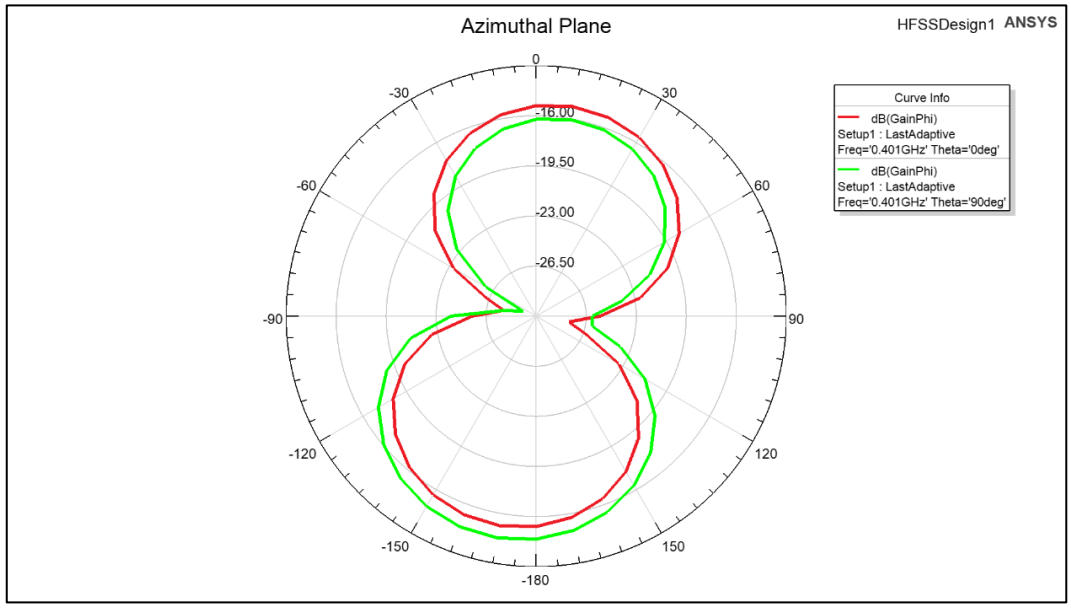

Figure 3.8 Azimuthal Plane

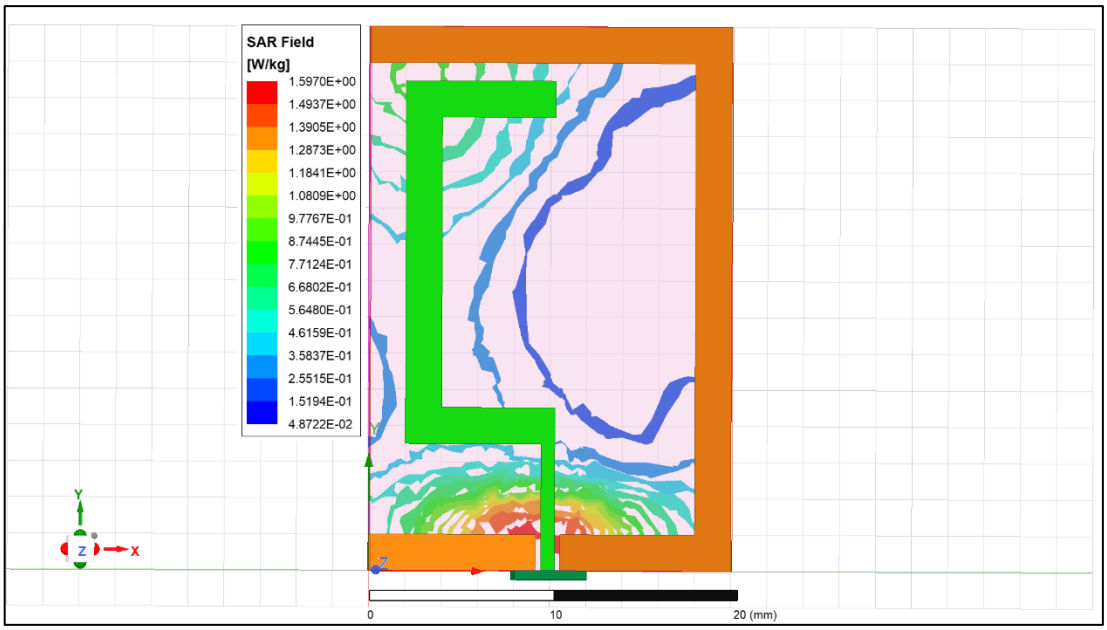

Figure 3.9 SAR field

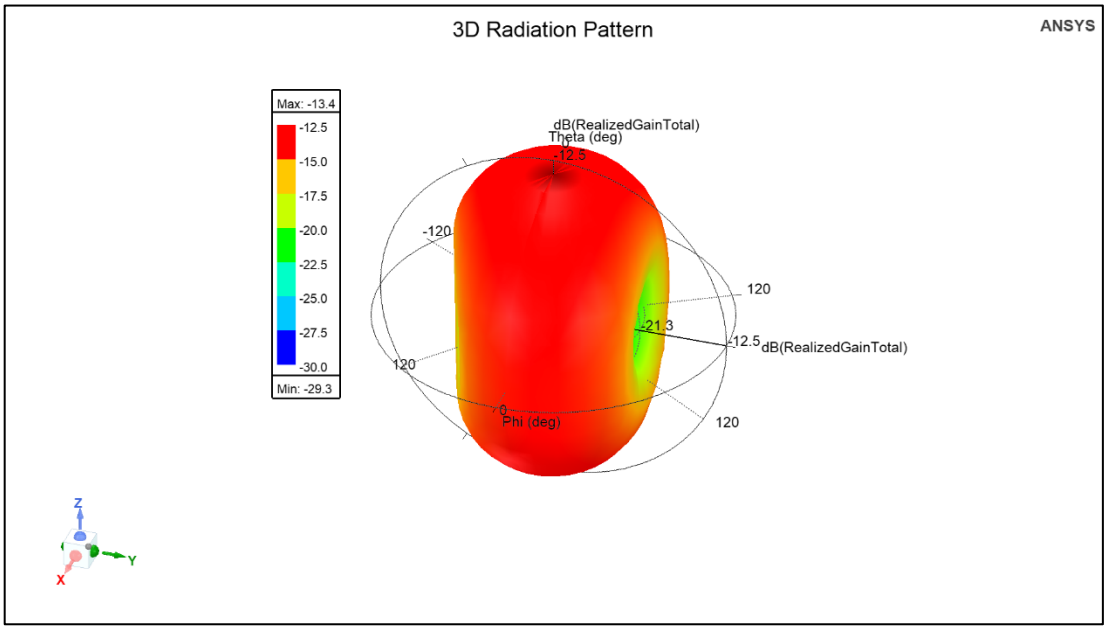

Figure 3.10 3D Radiation Pattern

At 433 MHz, it is evident that peak gain is -13.4 dBi. 2D radiation patterns are also observed. For input power of 10.3 mW, SAR value is 1.5937 W/kg which is considered safe (refer fig. 3.10 – 3.13).

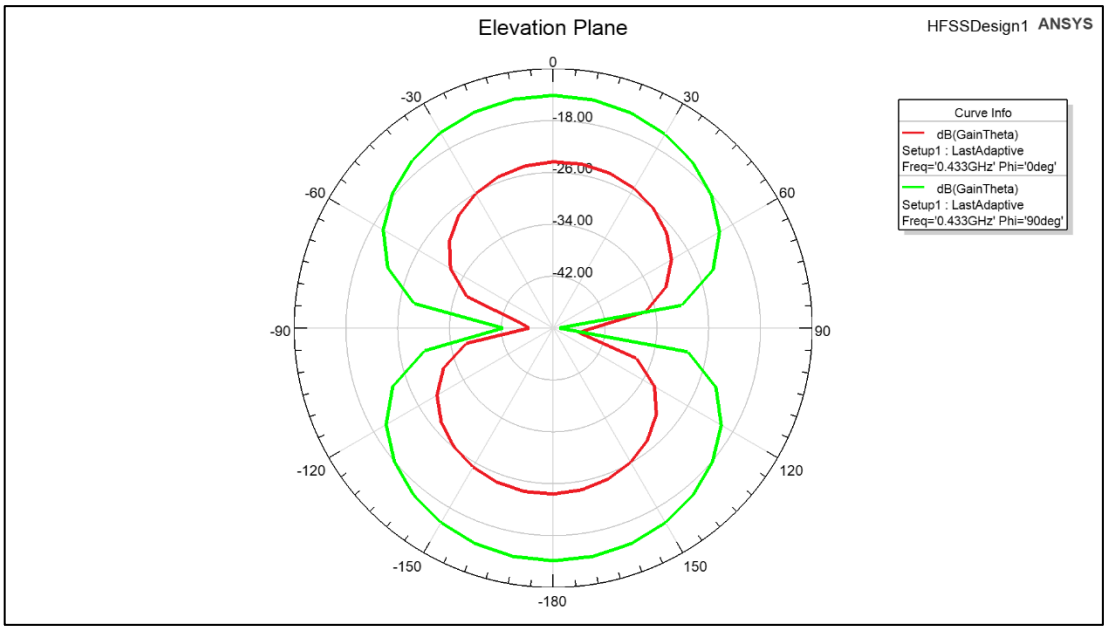

Figure 3.11 Elevation Plane

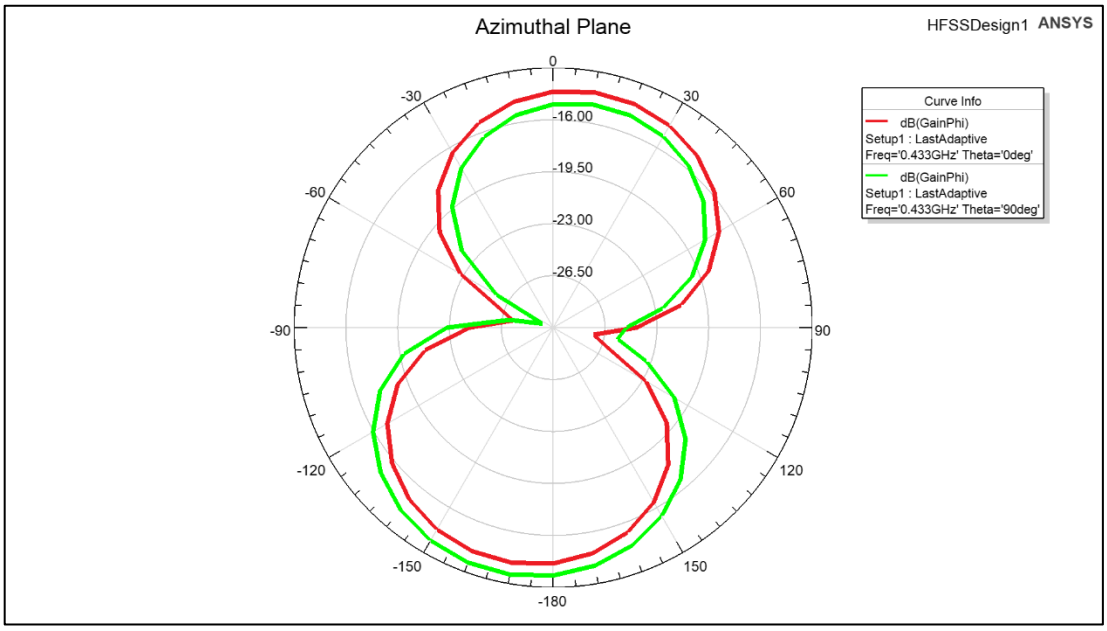

Figure 3.12 Azimuthal Plane

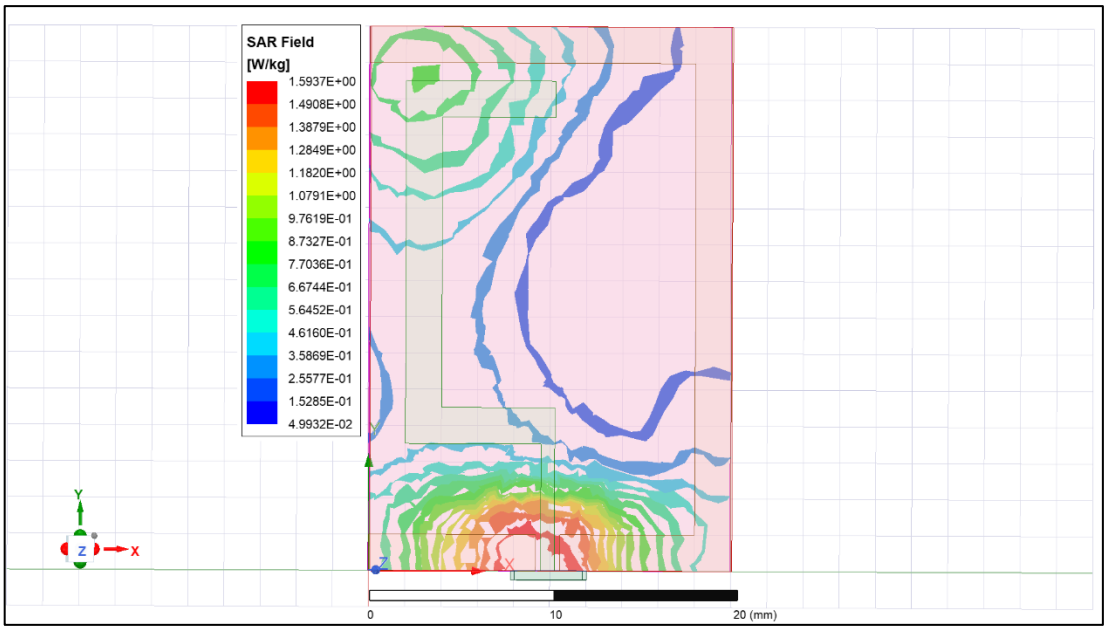

Figure 3.13 SAR field

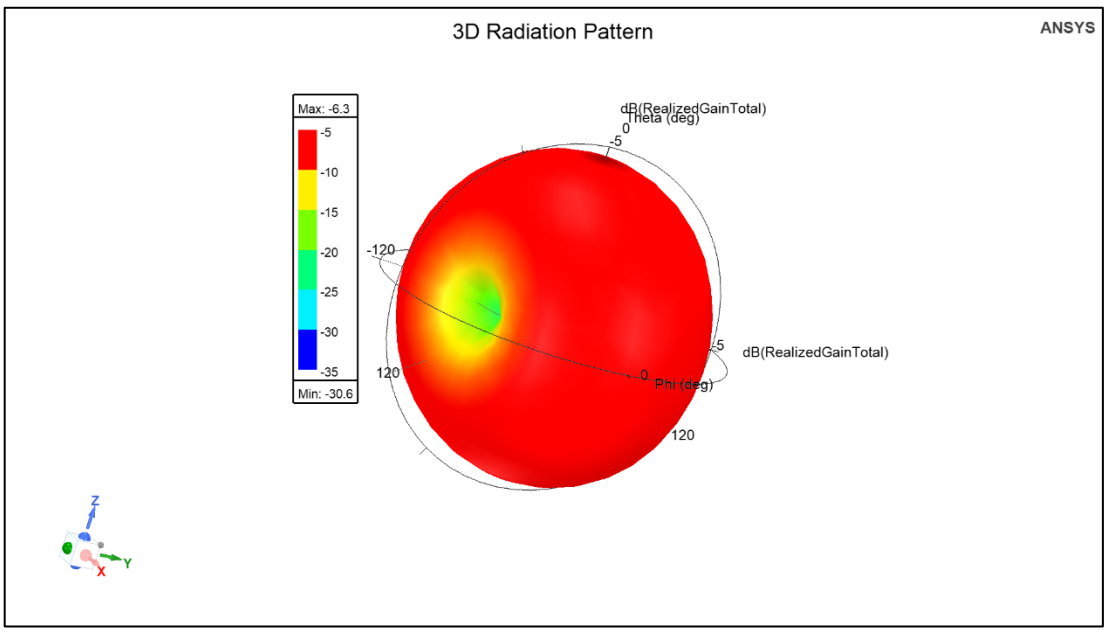

Figure 3.14 3D Radiation Pattern

At 865 MHz, it is evident that peak gain is -6.3 dBi. 2D radiation patterns are also observed. For input power of 22.2 mW, SAR value is 1.5948 W/kg which is considered safe (refer fig. 3.14 – 3.17).

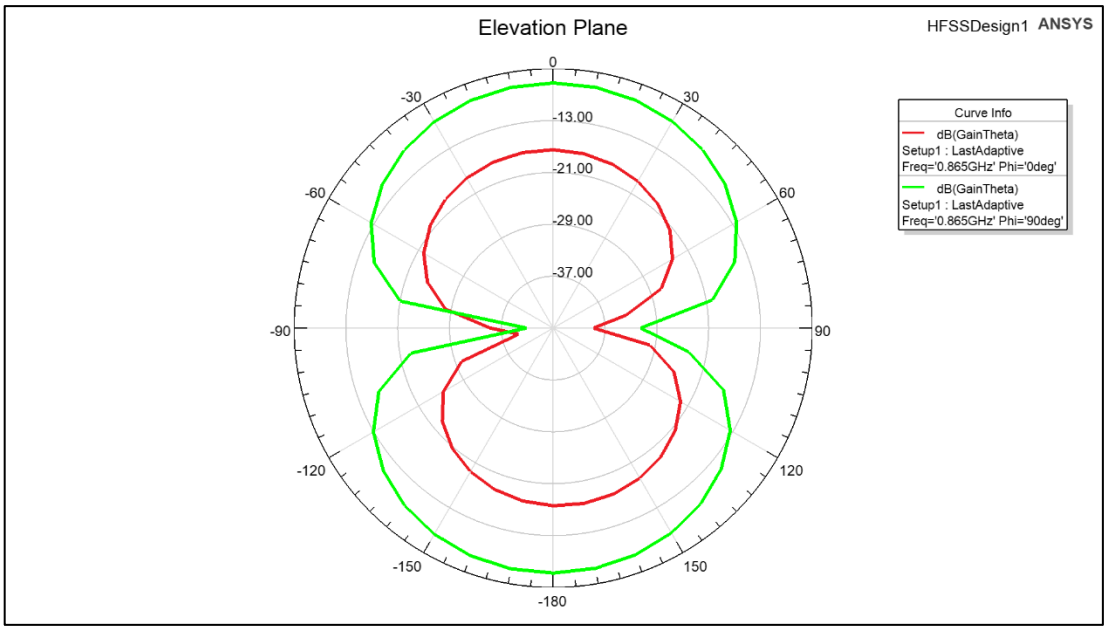

Figure 3.15 Elevation Plane

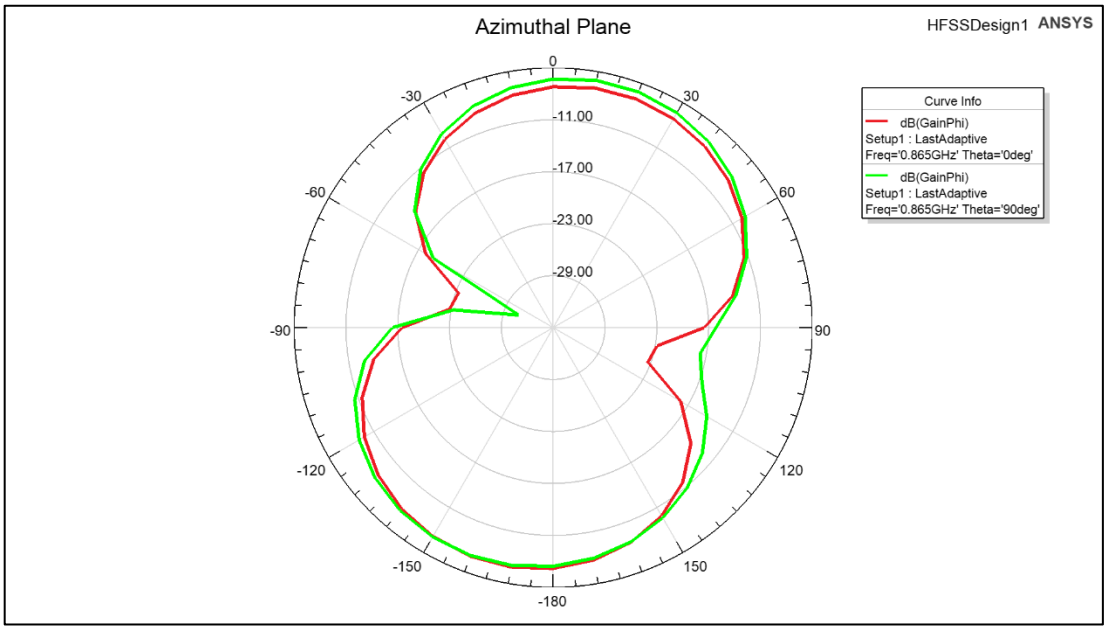

Figure 3.16 Azimuthal Plane

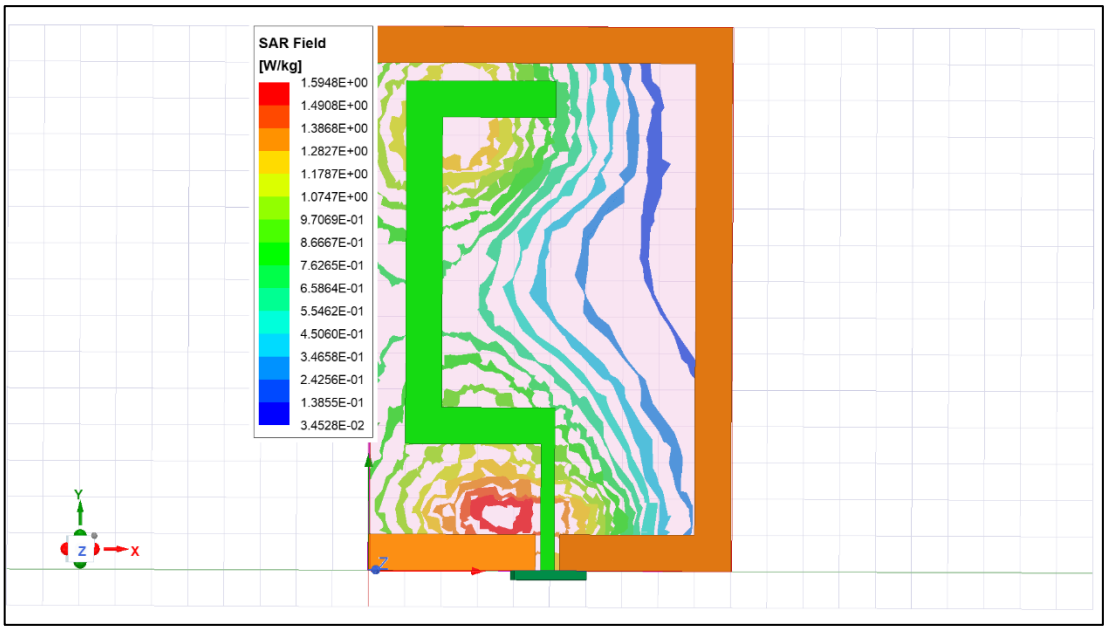

Figure 3.17 SAR field

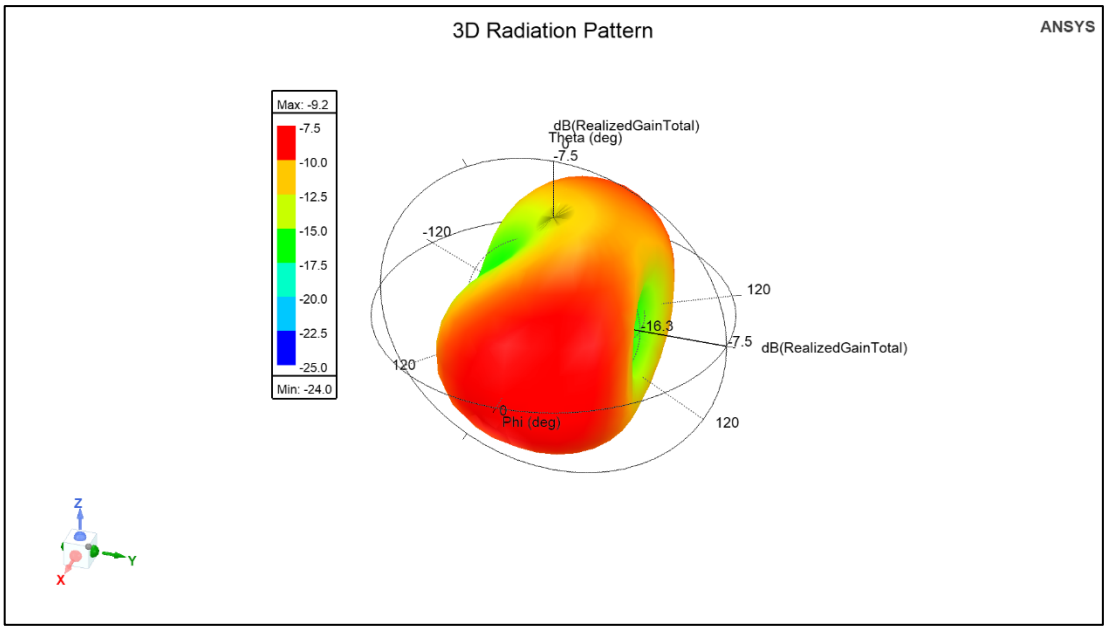

Figure 3.18 3D Radiation Pattern

At 1.427 GHz, it is evident that peak gain is -9.2 dBi. 2D radiation patterns are also observed. For input power of 19.5 mW, SAR value is 1.5961 W/kg which is considered safe (refer fig. 3.18 – 3.21).

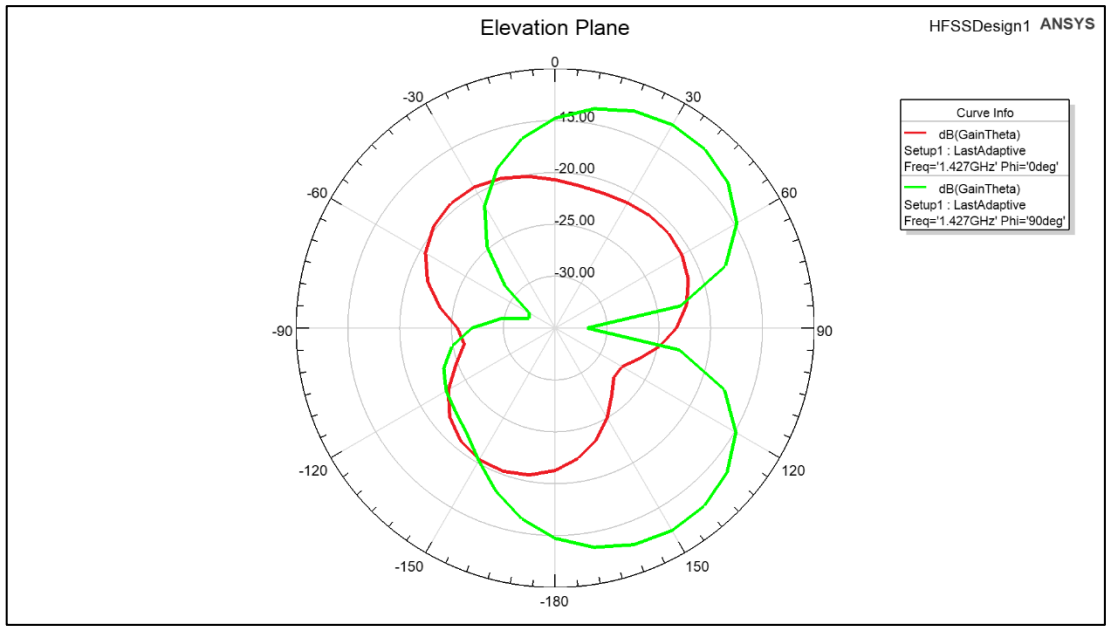

Figure 3.19 Elevation Plane

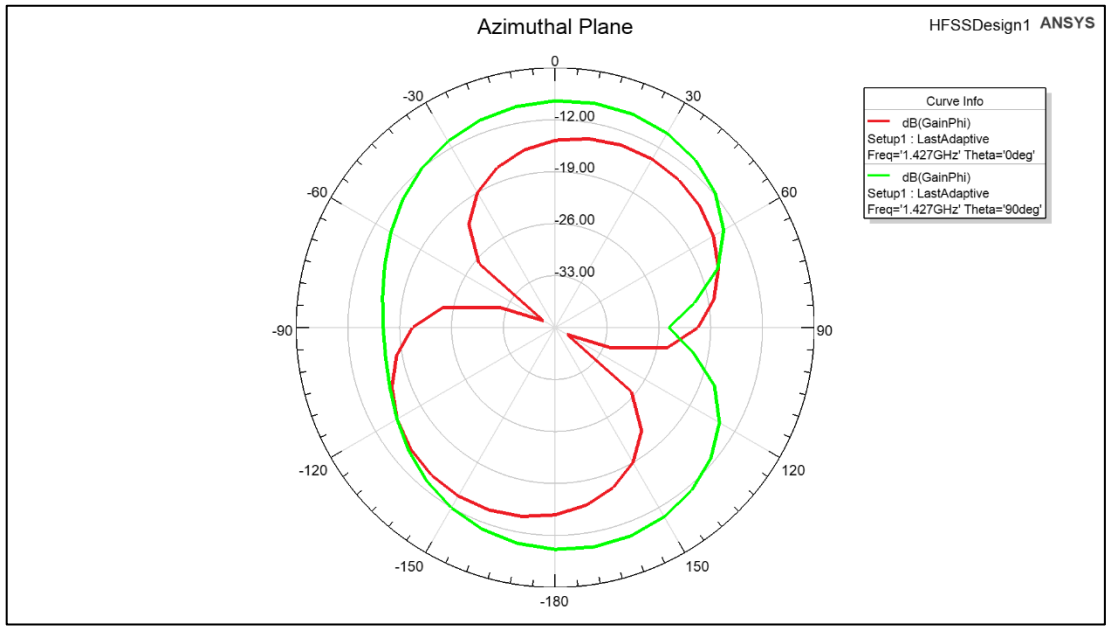

Figure 3.20 Azimuthal Plane

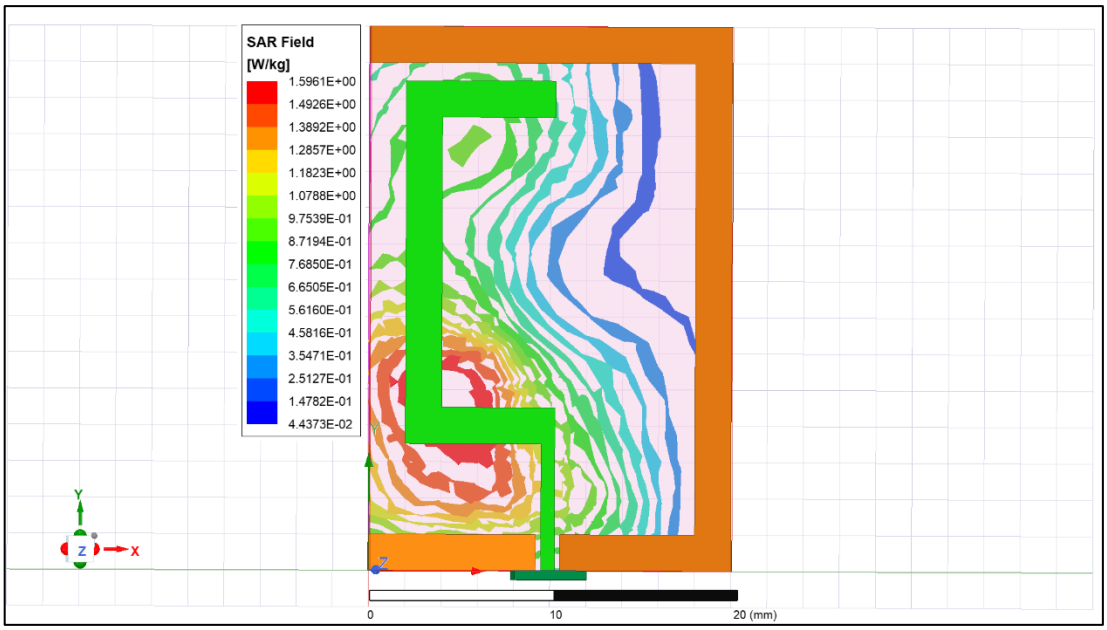

Figure 3.21 SAR field

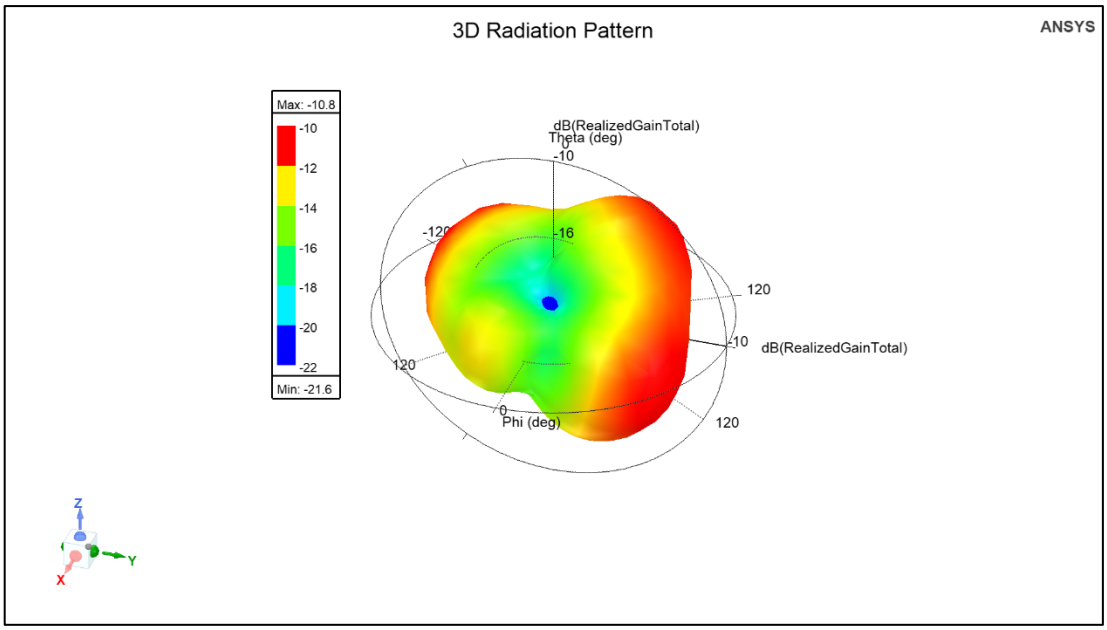

Figure 3.22 3D Radiation Pattern

At 2.4 GHz, it is evident that peak gain is -10.8 dBi. 2D radiation patterns are also observed. For input power of 18.2 mW, SAR value is 1.5949 W/kg which is considered safe (refer fig. 3.22 – 3.25).

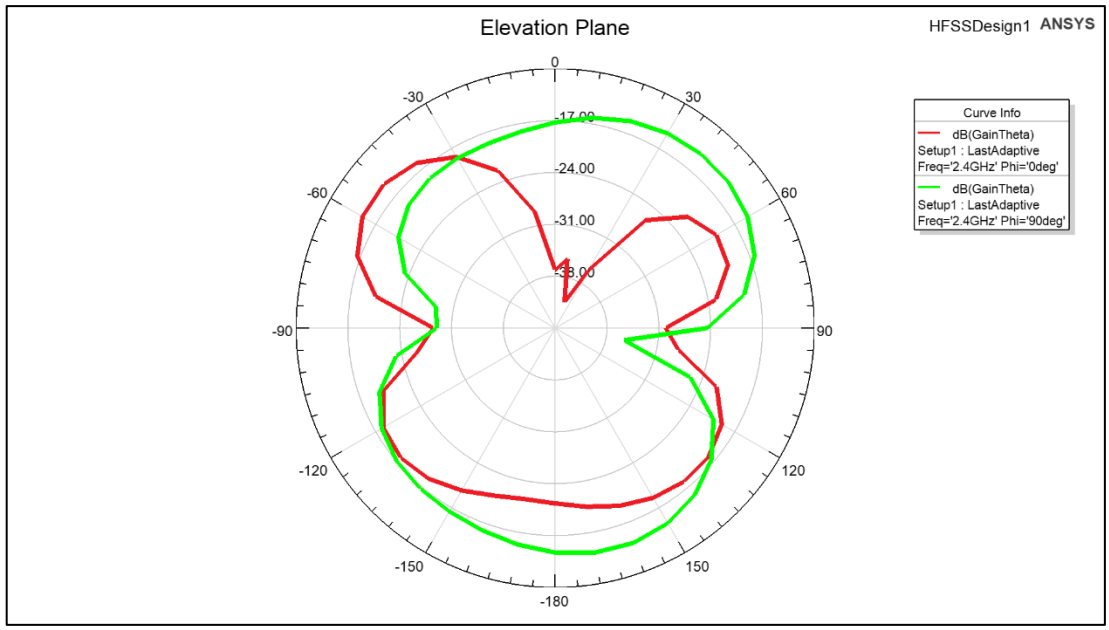

Figure 3.23 Elevation Plane

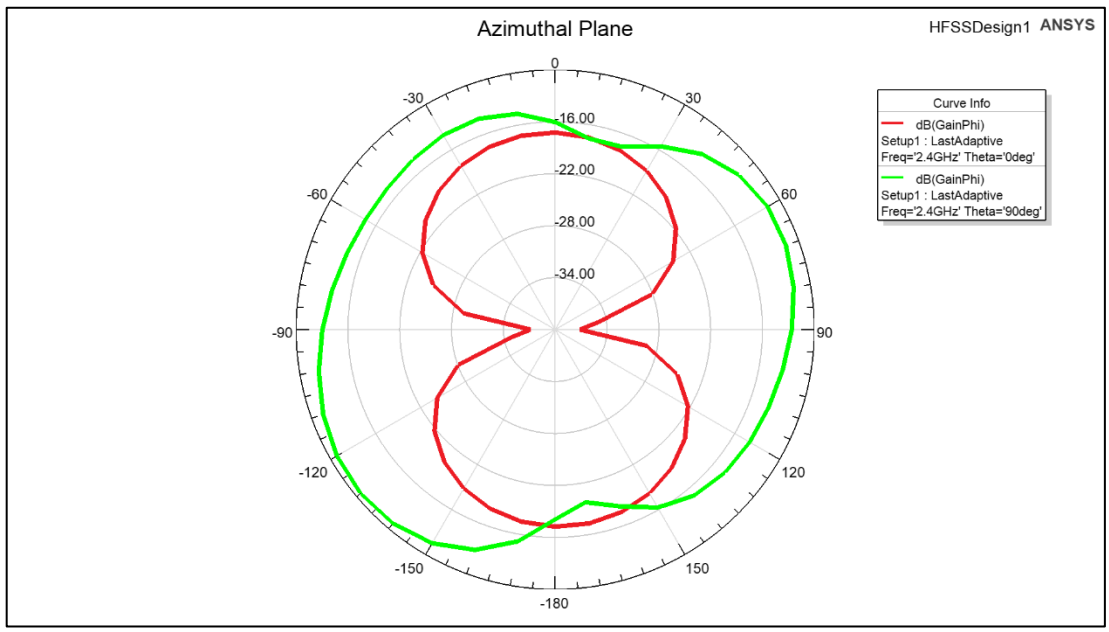

Figure 3.24 Azimuthal Plane

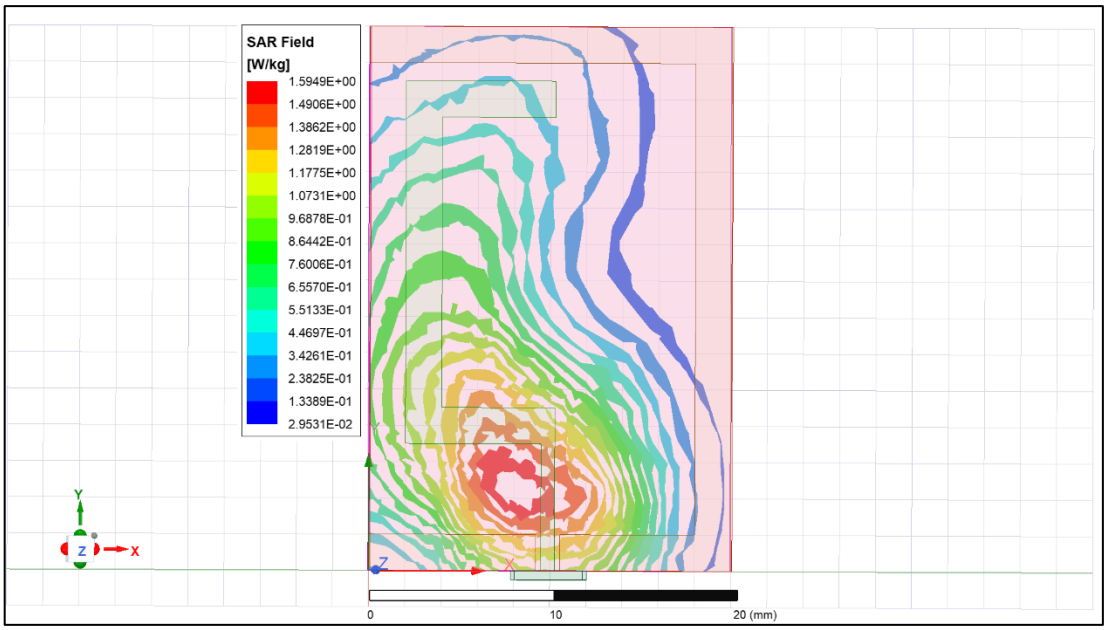

Figure 3.25 SAR field

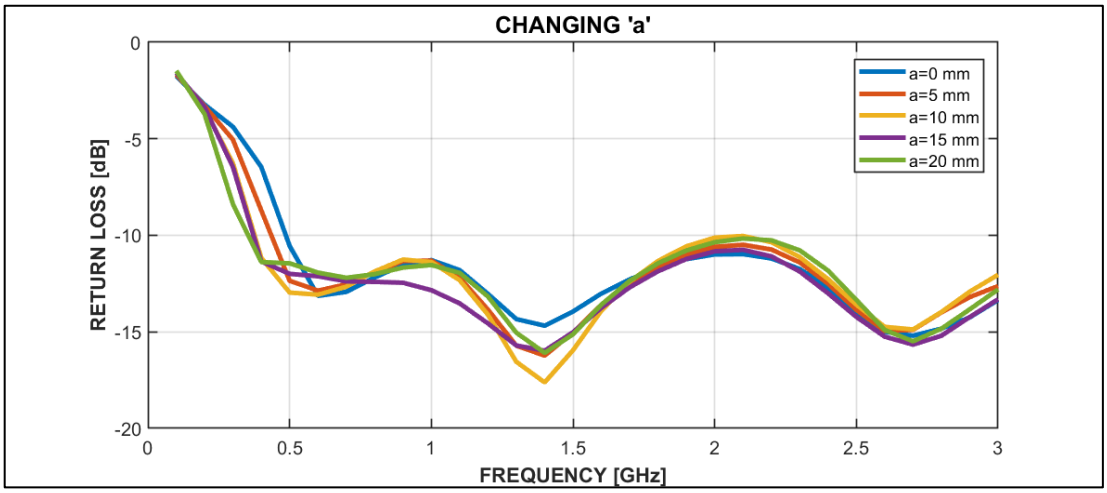

Figure 3.26 Return loss vs Frequency

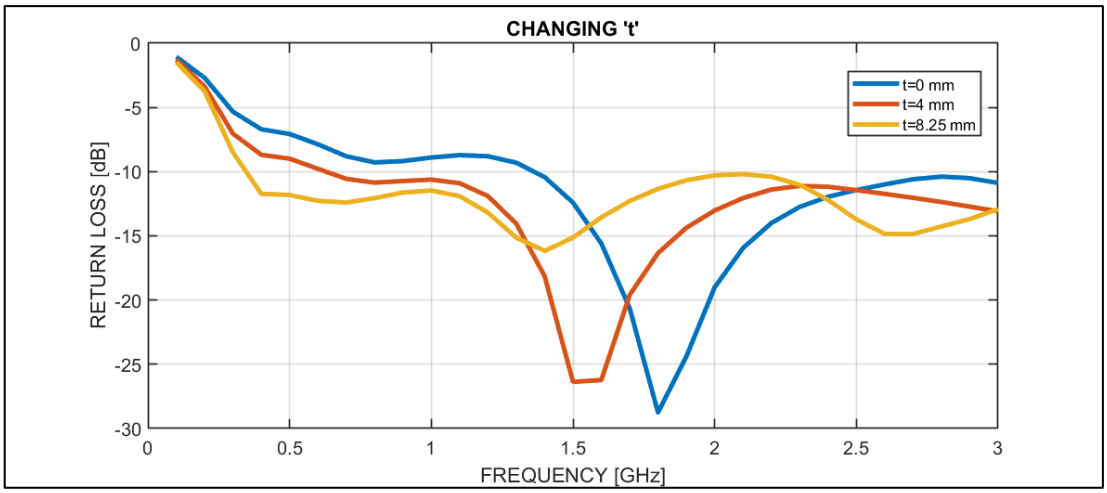

Figure 3.27 Return loss vs Frequency

We have observed in fig. 3.26 that for values of parameter 'a' to be 0 mm, 5 mm, 10 mm and 15 mm, the antenna does not operate at all the frequency bands. Also, as depicted in fig. 3.27 by changing the parametric values of 't' to 0 mm and 4 mm, the antenna does not work at all frequency bands that we intend to.

3.2 BIOCOMPATIBLE IMPLANTABLE ANTENNA

Here the antenna, as discussed in section 3.1, operates at all the biomedical frequency bands i.e., MedRadio, MICS, WMTS and ISM bands. With the help of AEDT simulation software, this implantable antenna is designed which operates at the frequency bands mentioned above. For the simulation setup, multiple frequencies- 401 MHz, 433 MHz, 865 MHz, 1.427 GHz and 2.4 GHz are selected. The antenna comprises of a rectangular C-shaped radiator patch, and an inverted rectangular C-shaped ground plane in a single layer as shown in fig 3.1 as well as fig. 3.3. The antenna design is same as discussed in the section 3.2 but here polyamide ($\varepsilon_r = 4.3$) is used as substrate while alumina ceramic ($\varepsilon_r = 9.8$) is used as superstrate. To attain perfect impedance matching, CPW technique is used. In this paper, the $20 \times 30 \times 1.6$ mm^3 antenna is positioned at the center of a $70 \times 70 \times 70$ mm^3 container which is filled

up with pork tissue to present an ideal body environment. Table I displays the measurements of the proposed antenna structure.

3.2.1 Results

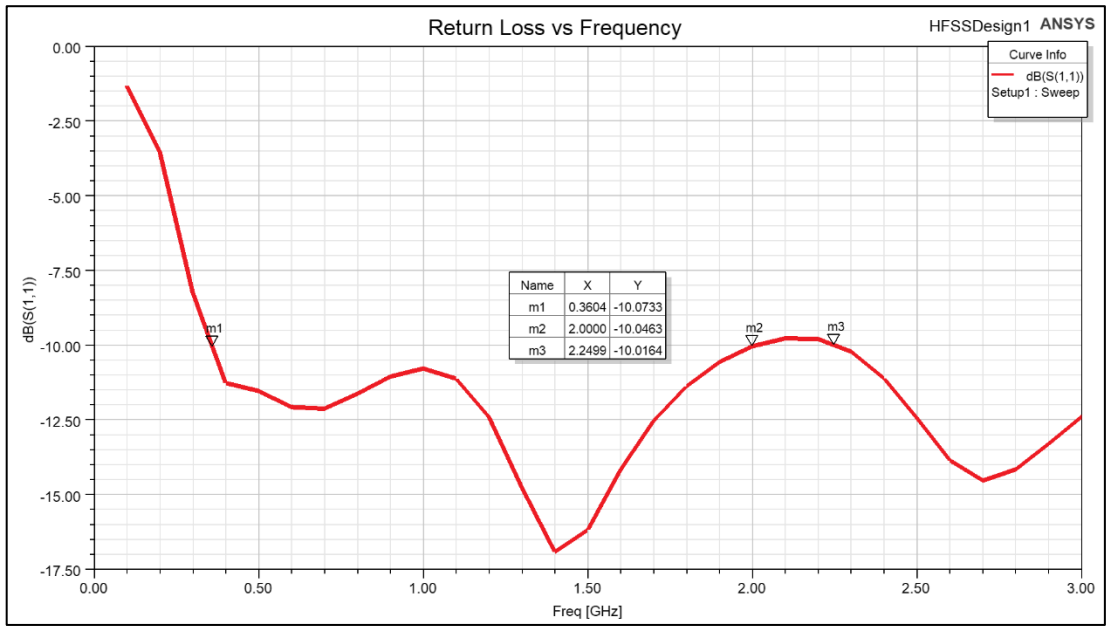

Figure 3.28 Return loss vs Frequency

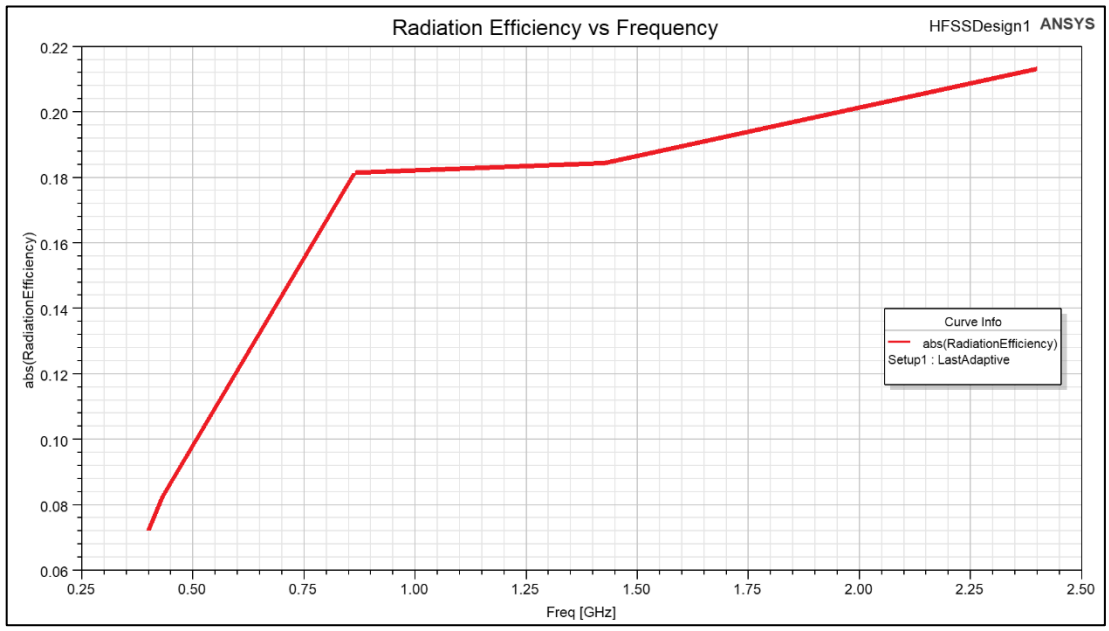

Figure 3.29 Radiation Efficiency vs Frequency

It is observed from fig. 3.28 that the antenna behaves as a wideband antenna as it resonates from 360.4 MHz to 2 GHz and beyond 2.2499 GHz, so it covers MICS band, MedRadio band, 433MHz ISM band, 865 MHz band, WMTS band, and 2.4 GHz ISM band. Radiation efficiency of the antenna increases with frequency (see fig. 3.29).

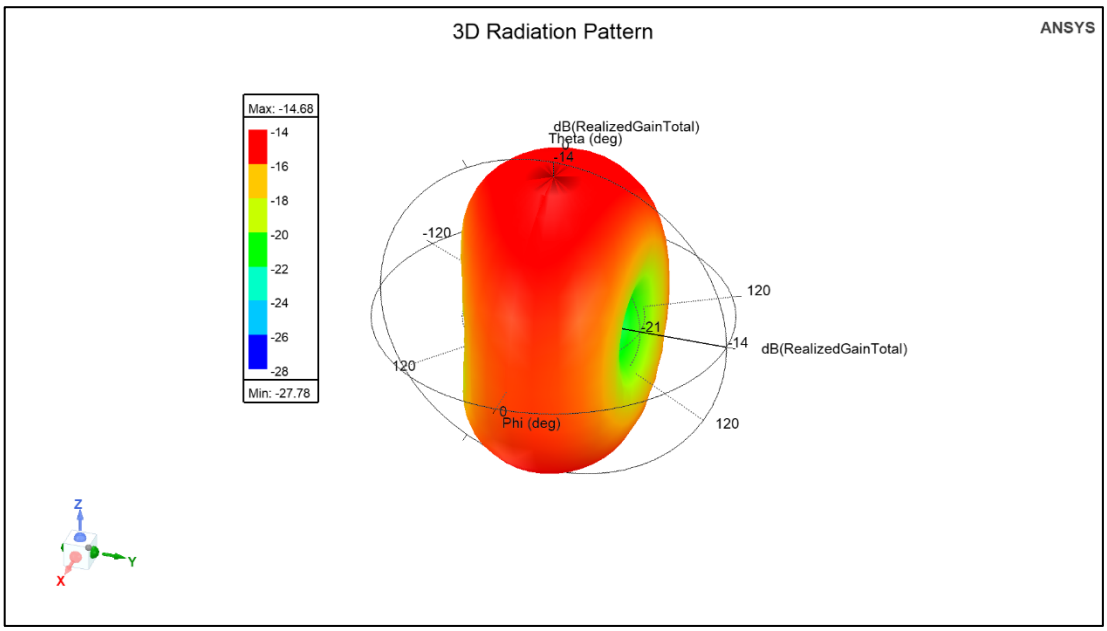

Figure 3.30 3D Radiation Pattern

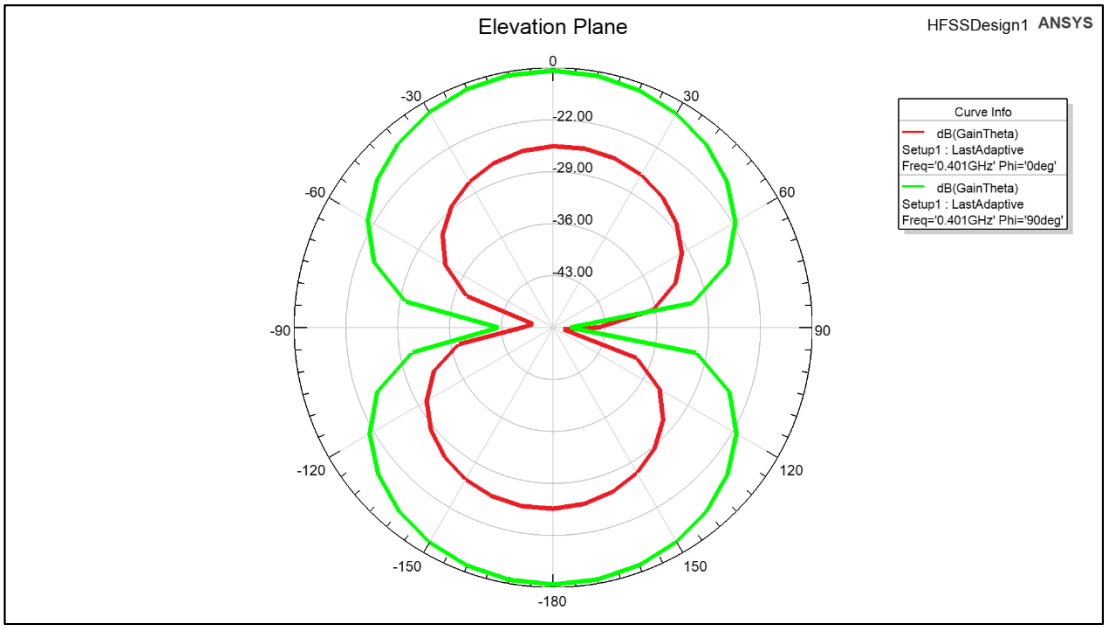

Figure 3.31 Elevation Plane

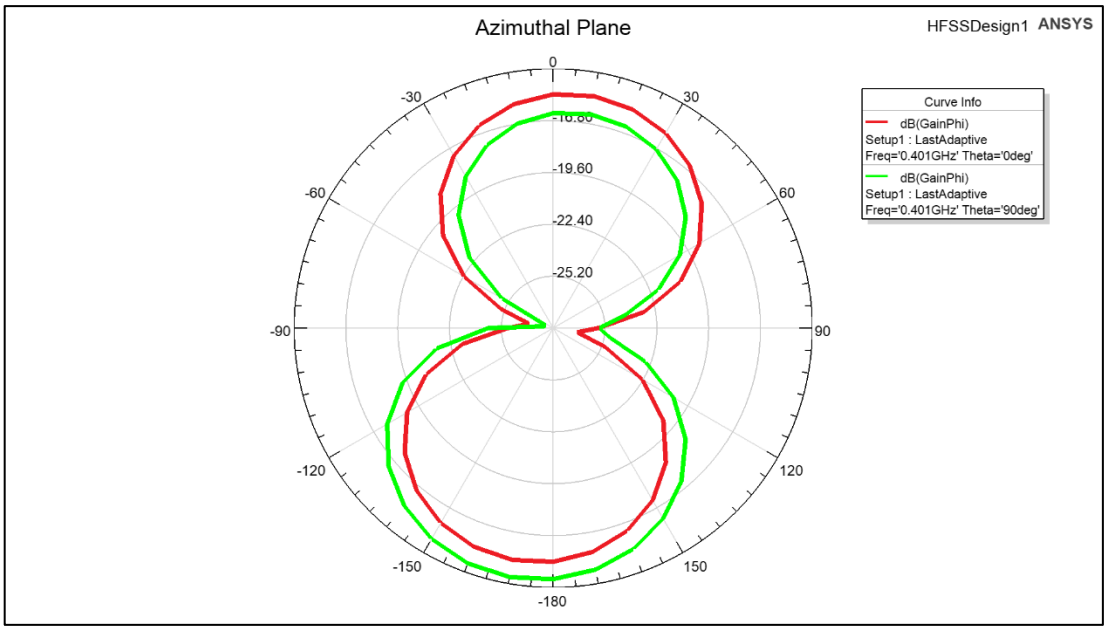

Figure 3.32 Azimuthal Plane

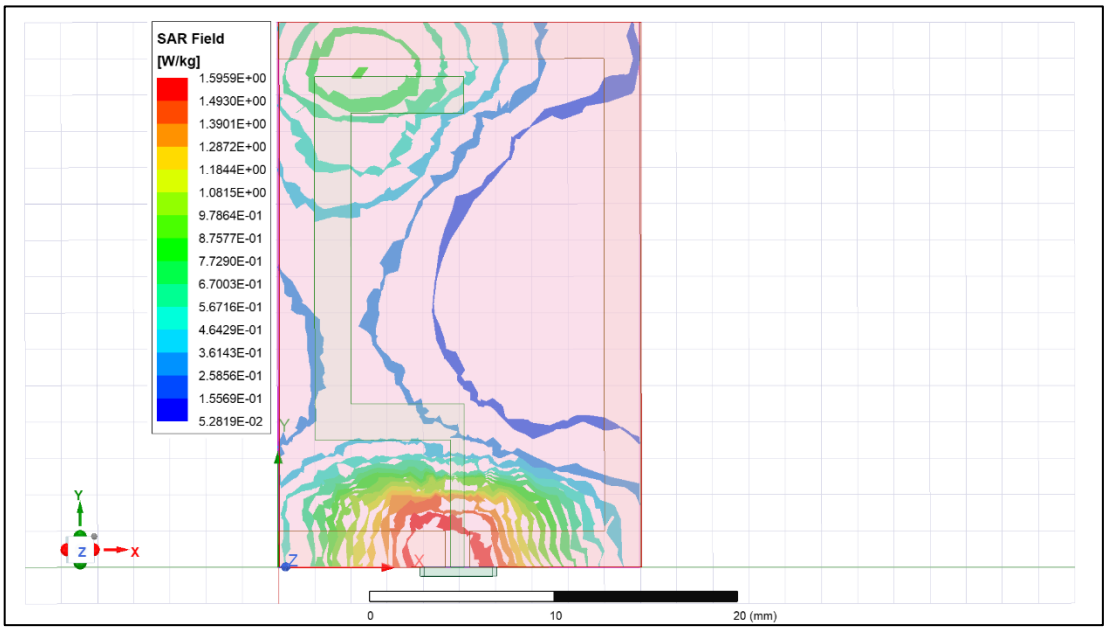

Figure 3.33 SAR field

At 401 MHz, it is evident that peak gain is -14.68 dBi. 2D radiation patterns are also observed. For input power of 9 mW, SAR value is 1.5959 W/kg which is considered safe (refer fig. 3.30 – 3.33).

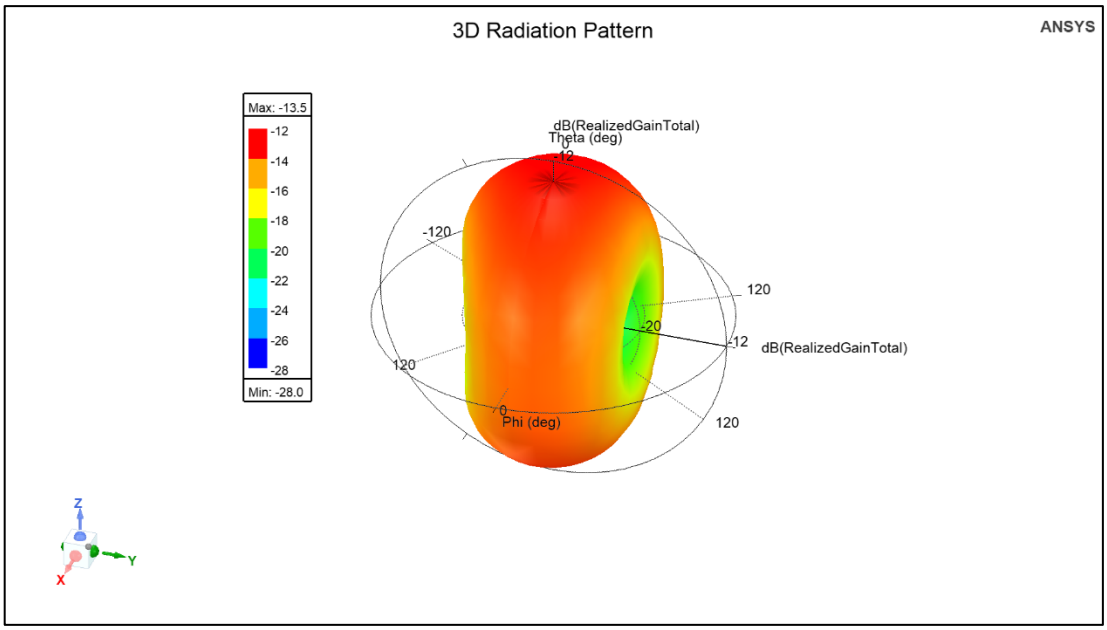

Figure 3.34 3D Radiation Pattern

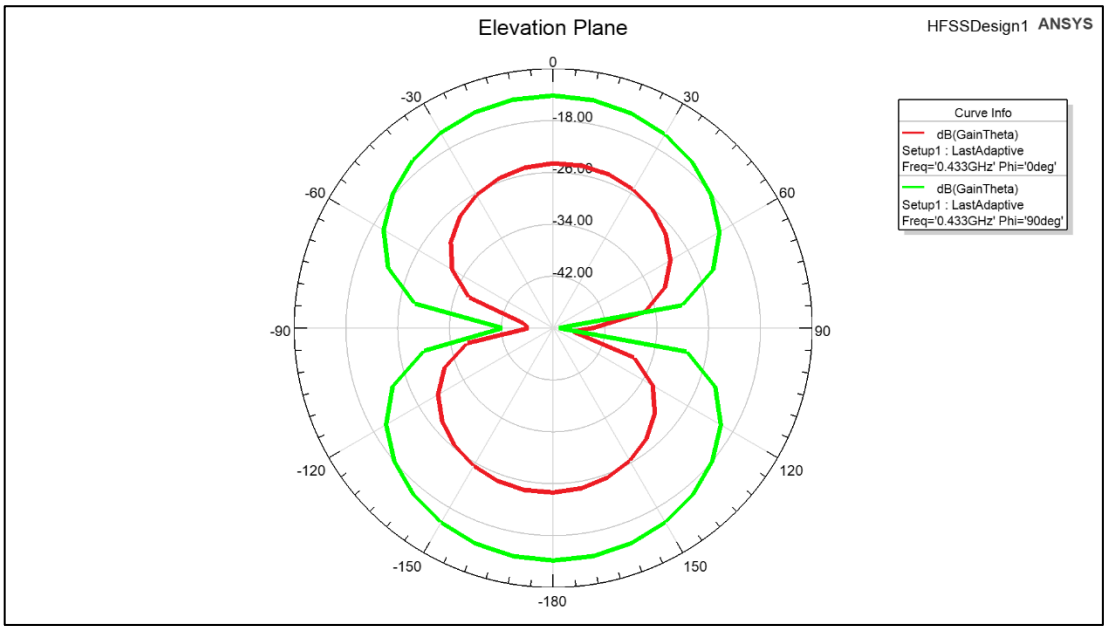

Figure 3.35 Elevation Plane

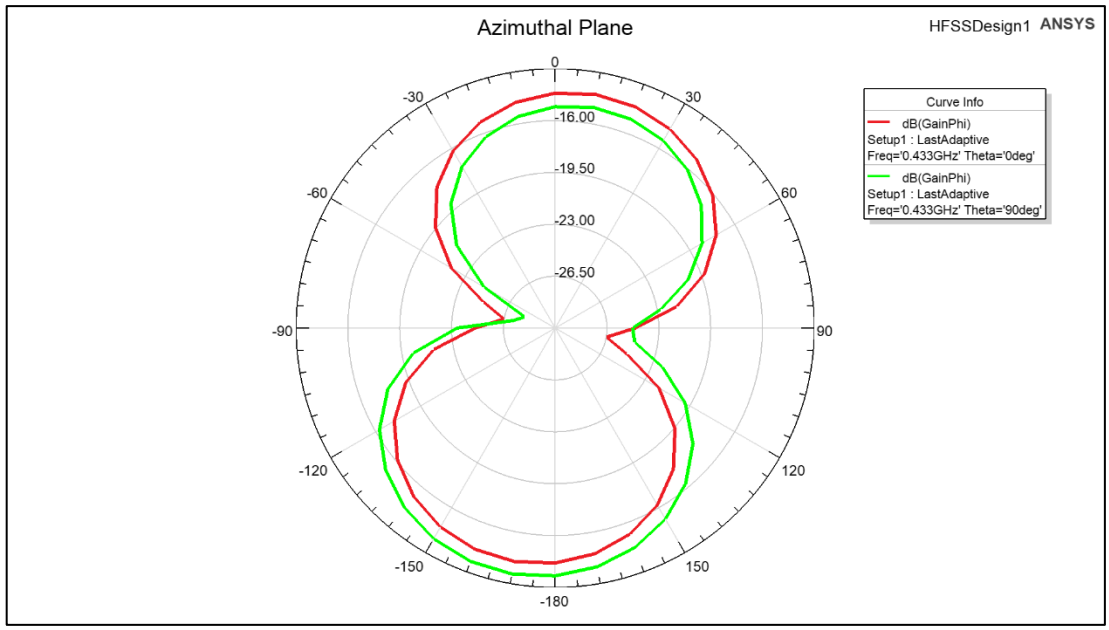

Figure 3.36 Azimuthal Plane

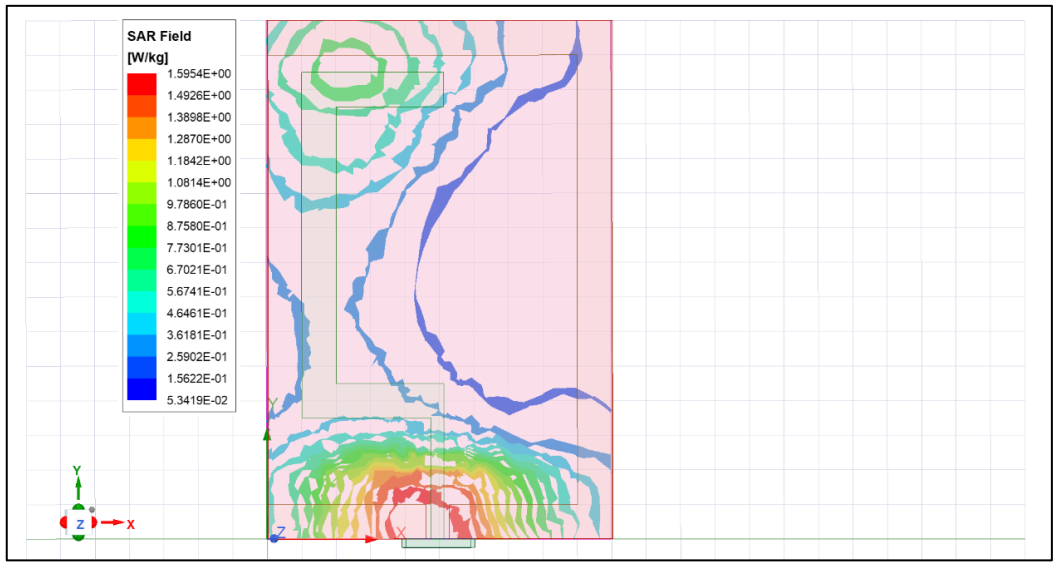

Figure 3.37 SAR field

At 433 MHz, it is evident that peak gain is -13.5 dBi. 2D radiation patterns are also observed. For input power of 9.2 mW, SAR value is 1.5954 W/kg which is considered safe (refer fig. 3.34 – 3.37).

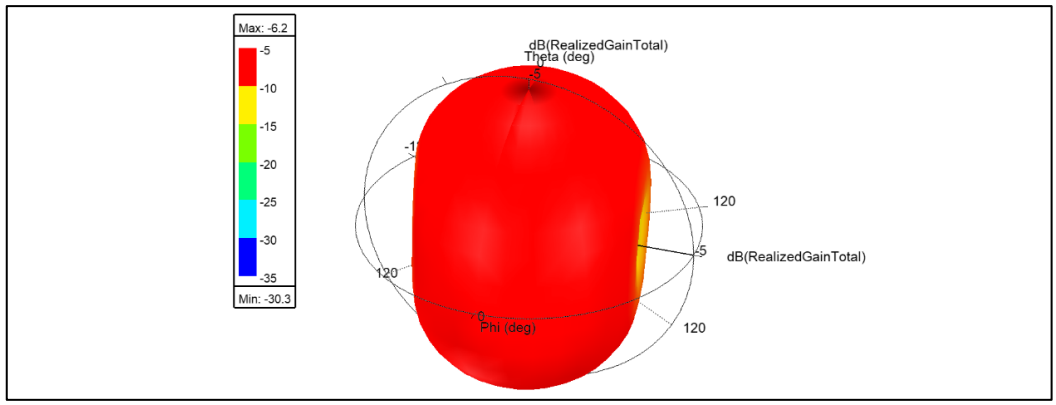

Figure 3.38 3D Radiation Pattern

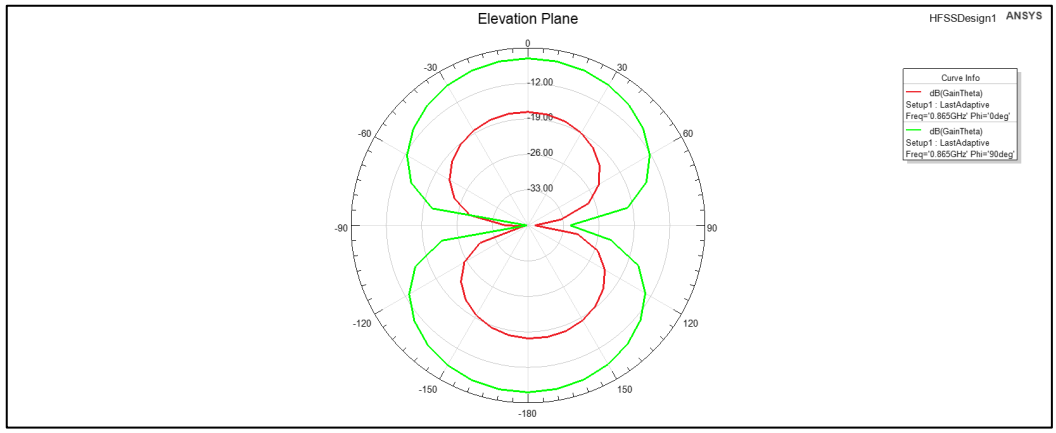

Figure 3.39 Elevation Plane

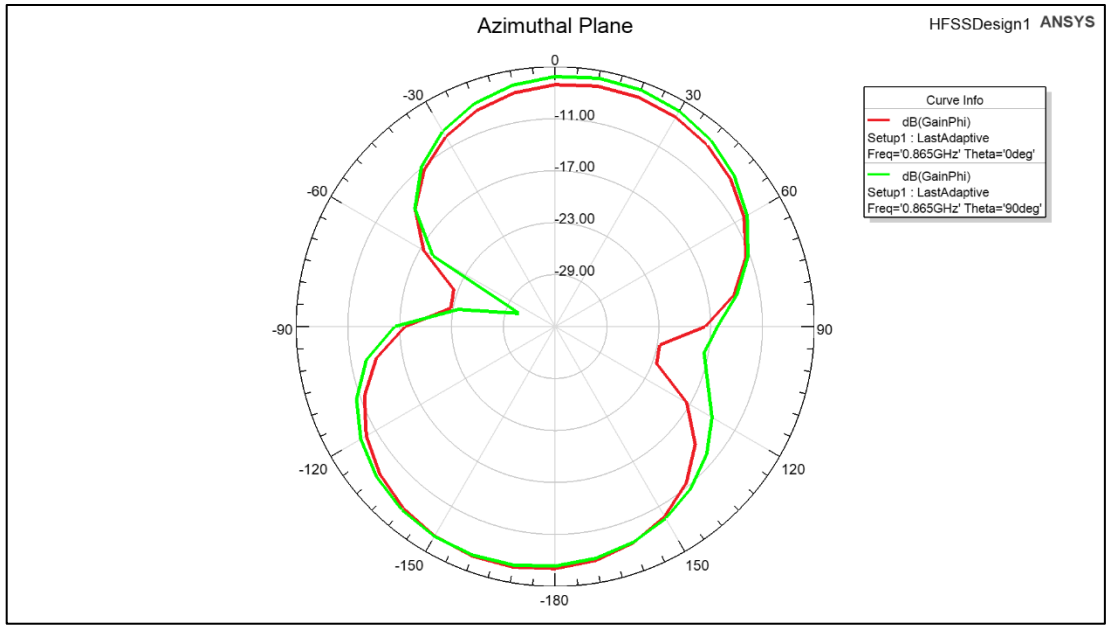

Figure 3.40 Azimuthal Plane

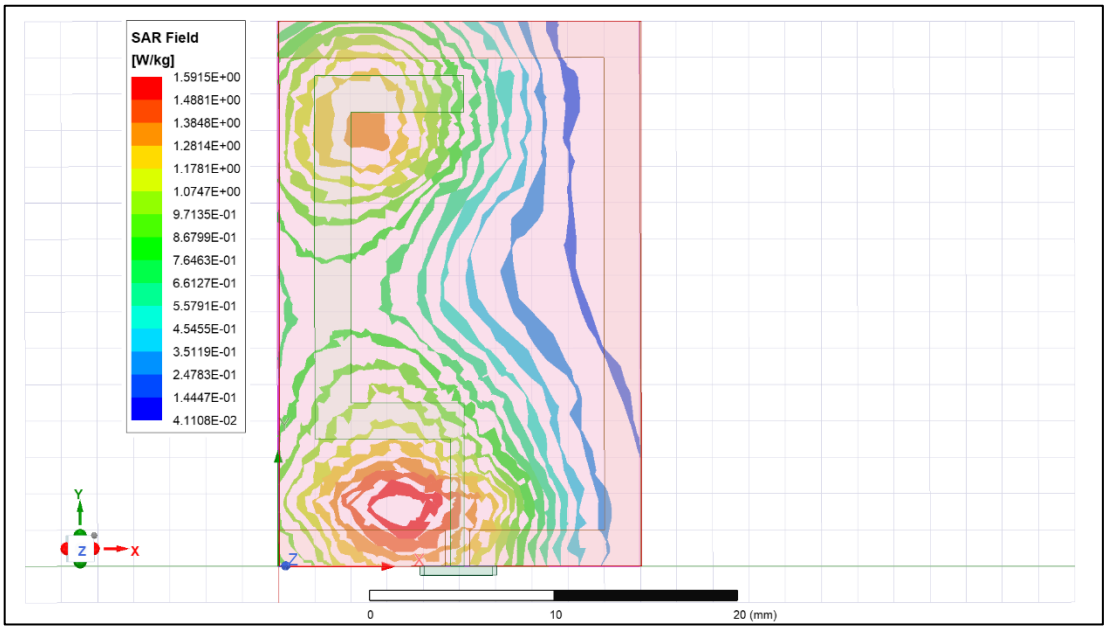

Figure 3.41 SAR field

At 865 MHz, it is evident that peak gain is -6.2 dBi. 2D radiation patterns are also observed. For input power of 23 mW, SAR value is 1.5915 W/kg which is considered safe (refer fig. 3.38 – 3.41).

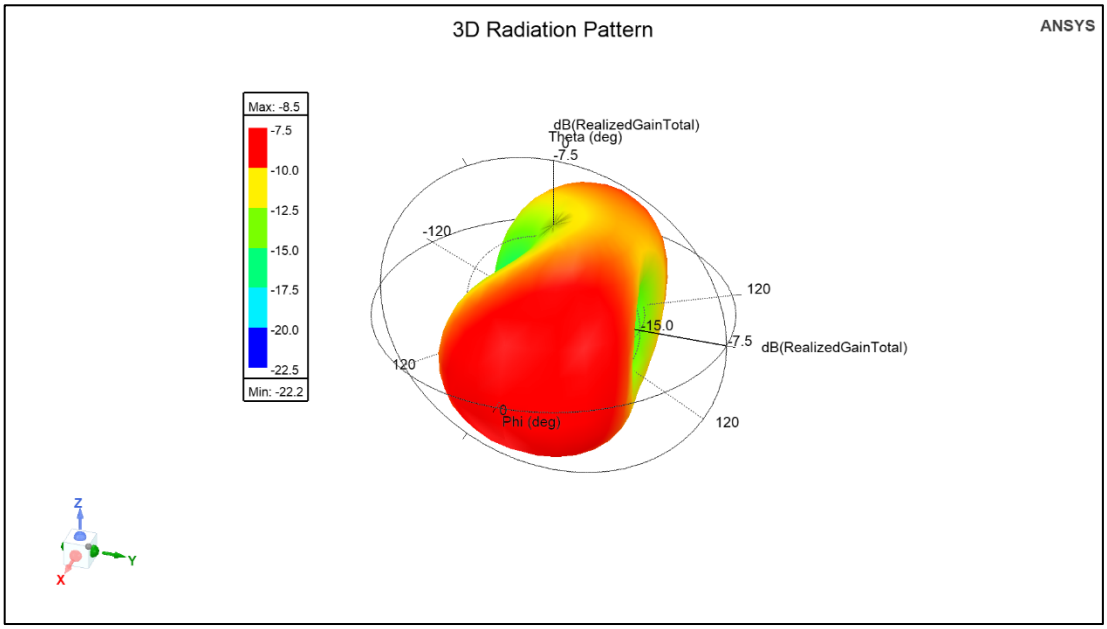

Figure 3.42 3D Radiation Pattern

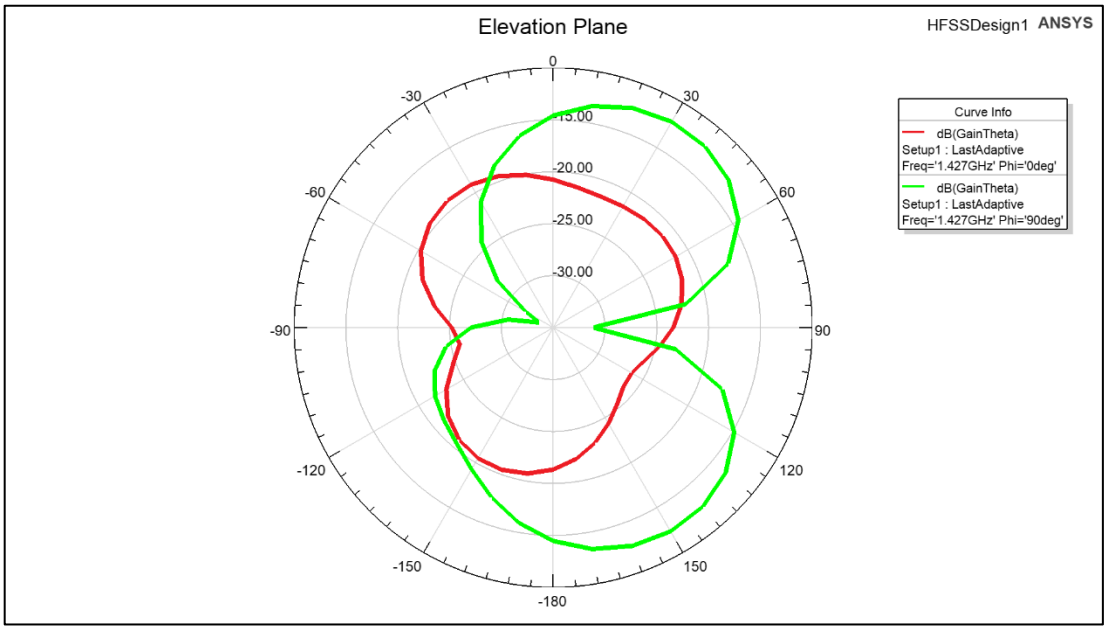

Figure 3.43 Elevation Plane

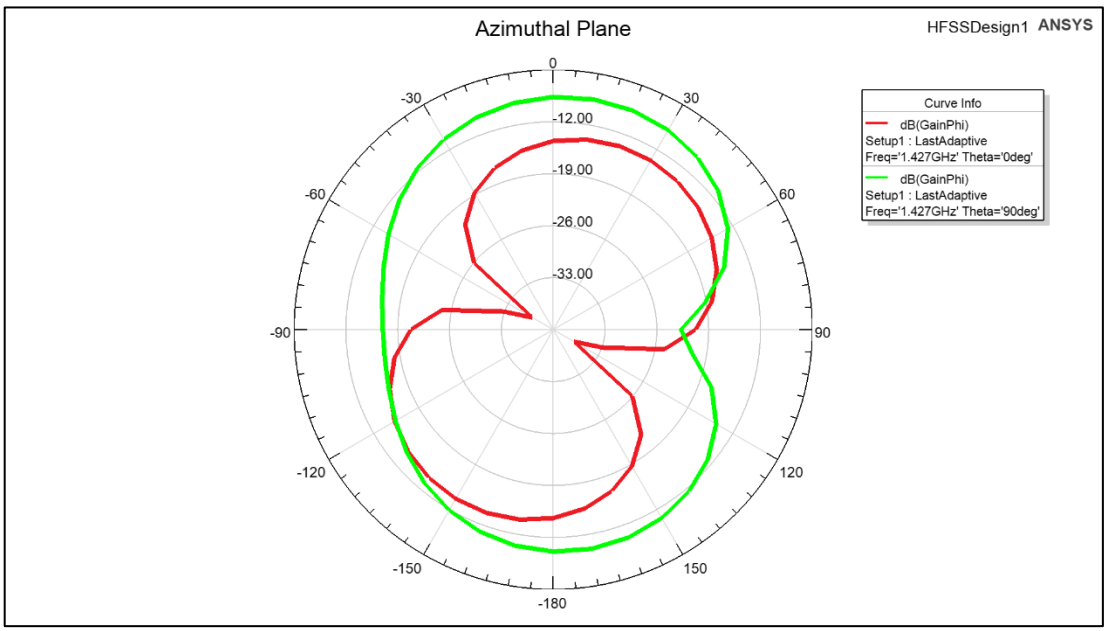

Figure 3.44 Azimuthal Plane

At 1.427 GHz, it is evident that peak gain is -8.5 dBi. 2D radiation patterns are also observed. For input power of 19.8 mW, SAR value is 1.5897 W/kg which is considered safe (refer fig. 3.42 – 3.45).

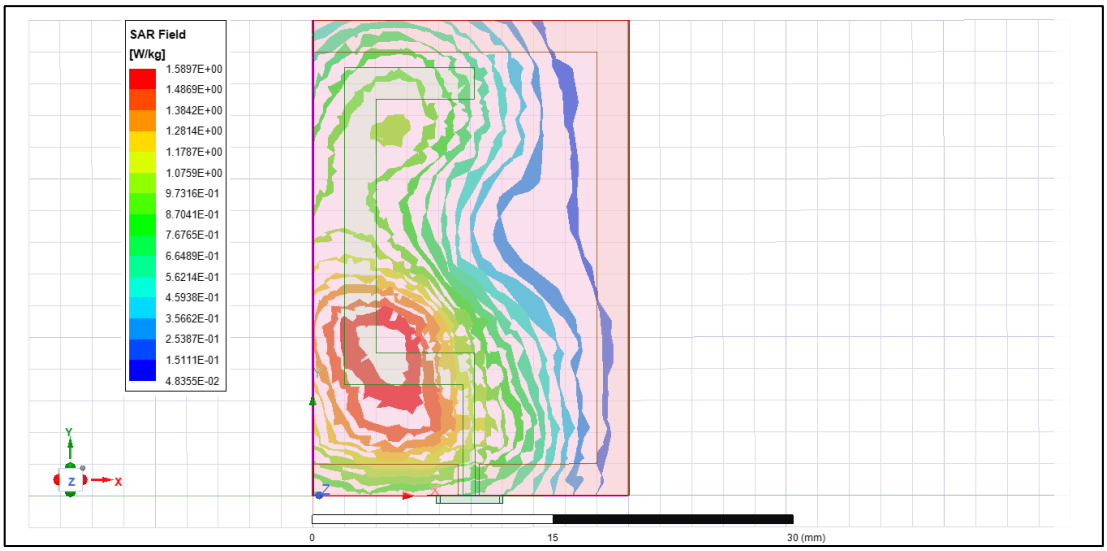

Figure 3.45 SAR field

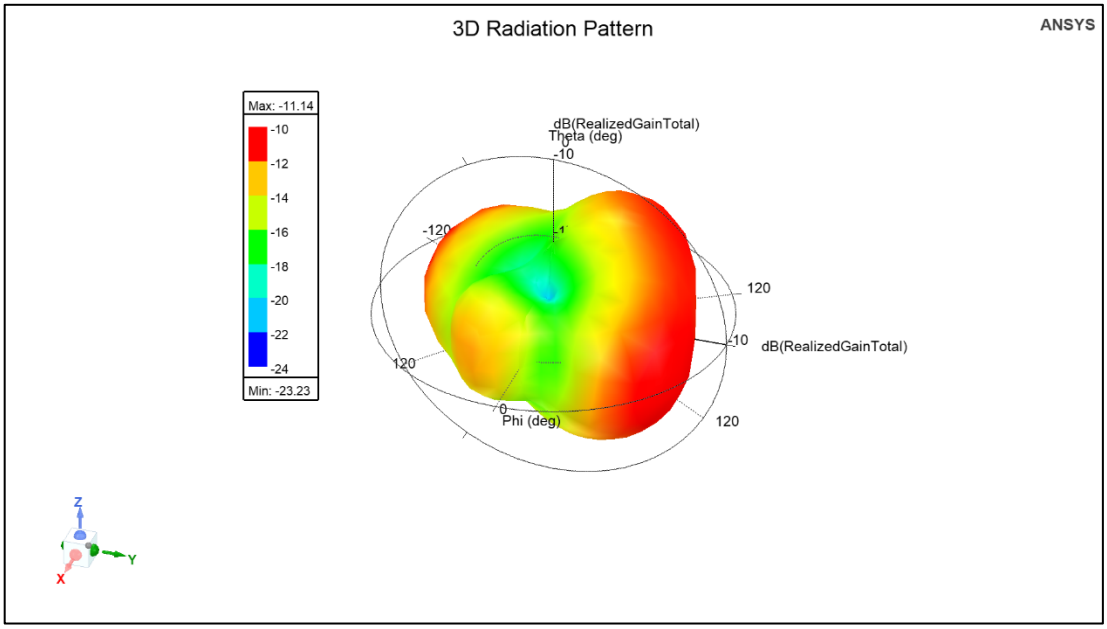

Figure 3.46 3D Radiation Pattern

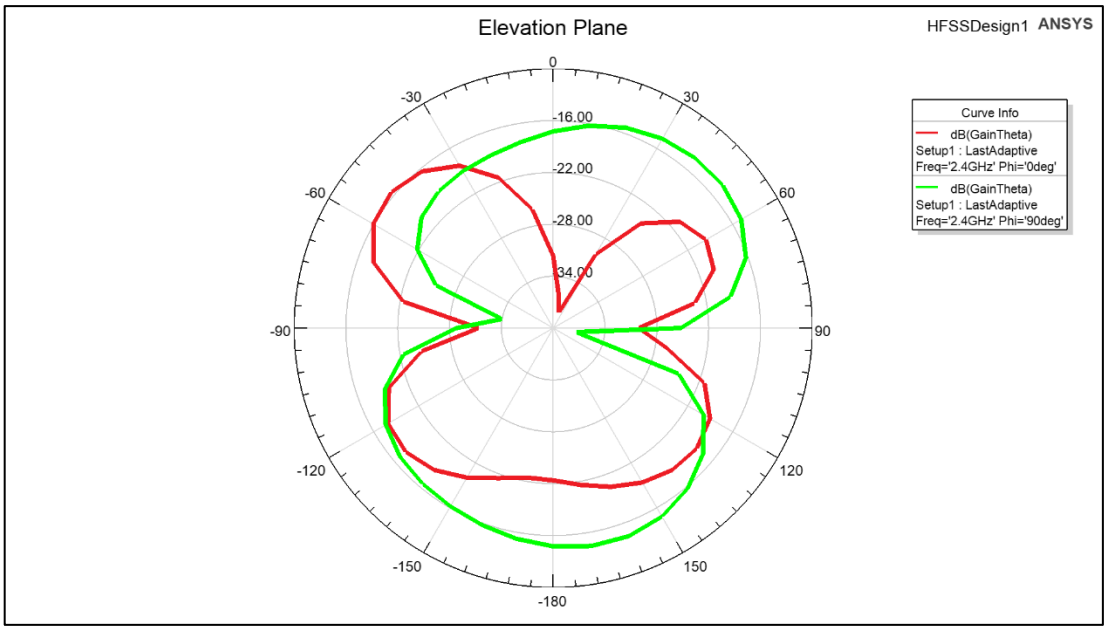

Figure 3.47 Elevation Plane

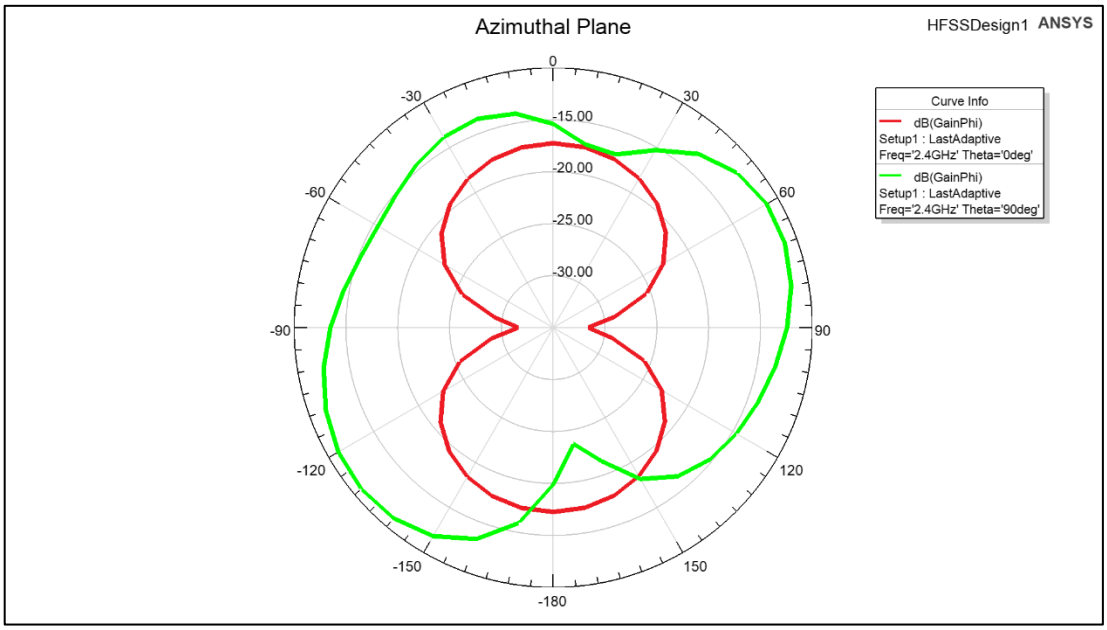

Figure 3.48 Azimuthal Plane

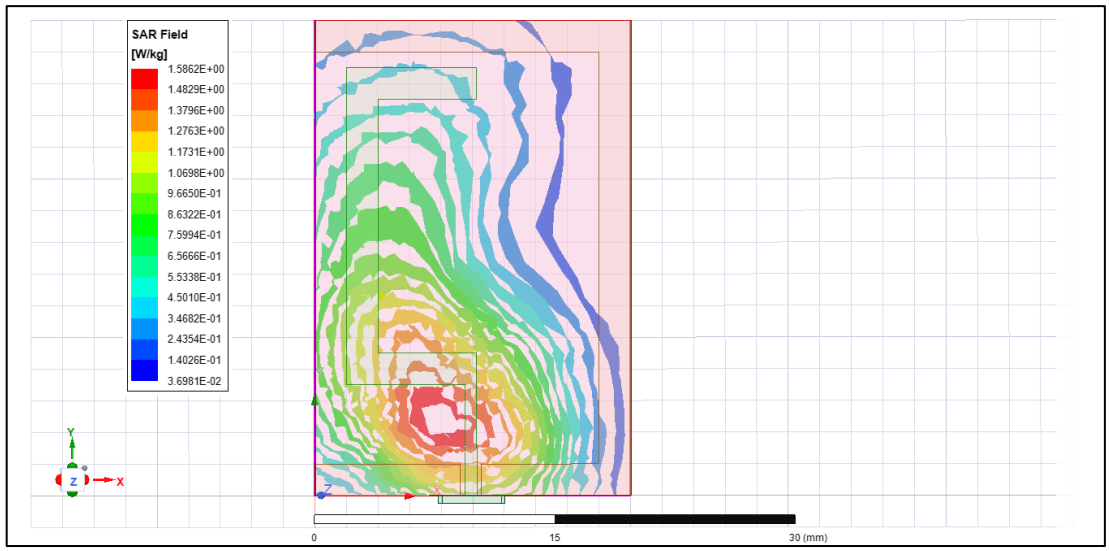

Figure 3.49 SAR field

At 2.4 GHz, it is evident that peak gain is -11.14 dBi. 2D radiation patterns are also observed. For input power of 18.3 mW, SAR value is 1.5862 W/kg which is considered safe (refer fig. 3.46 – 3.49).

CHAPTER 4

WCE CONFORMAL ANTENNA

For WCE, outer wall antennas are preferred, as they save space inside the capsule while providing greater performance than an antenna inside the capsule. Since the size of the capsule is so small electrically in comparison to the frequency range, the antenna design has a significant impact on the quality, energy efficiency, and form factor of the capsule. Furthermore, the capsule antenna must have wider bandwidth. As the capsule moves through the GI tract, the body tissue around it changes and so do the properties of tissues. Narrowband antennas can get detuned due to differences in material qualities. The use of ultra-wide bandwidth can serve to minimise detuning effects.

The dimensions of the capsule, as displayed in fig. 1.1, are 26 mm x 11 mm. The antenna conforms to the surface of the capsule, which has a cylindrical shape (radius of 5.5 mm and height of 15 mm) and a Teflon substrate ($\varepsilon_r = 2.1$, $\tan \delta = 0.001$) of height 0.8 mm, to maximise the usage of space inside the capsule. To maintain biocompatibility Ultem ($\varepsilon_r = 3.05$, $\tan \delta = 0.006$) is used to make the 0.5 mm thick capsule [14,15]. The capsule cylinder is hollow. Blood, muscle, bone, and fat are dielectric and conductivity materials with varying dielectric and conductivity properties inside the human body. This results in a very complex electromagnetic structure to model and design, as well as a significant computational load, which

lengthens simulation time. Thereby, in this paper, a homogeneous human body phantom has been used (ε_r = 56 and σ = 0.8 S/m) to replicate the environment inside the human body [7].

4.1 ANTENNA-1

A simple T-shaped structure is taken as the radiator as shown in fig. 4.1. Then the antenna is conformed around the exterior of the capsule (see fig. 4.3). The parametric measurements of the antenna are discussed in Table II. The radiator is metal, and it is harmful to the body upon exposure, so zirconia can be used for bio-encapsulation.

4.1.1 Planar design

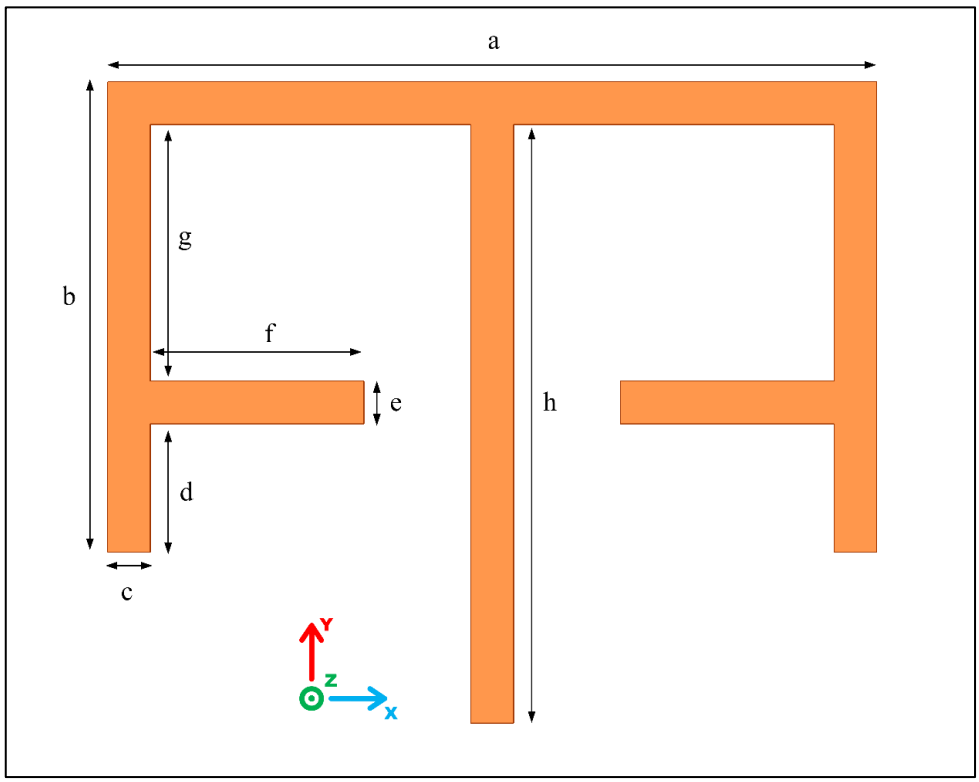

Figure 4.1 Planar design of antenna

Table II. Dimensions of antenna

DIMENSIONS	VALUE (mm)
a	18
b	11
c	1
d	3
e	1
f	5
g	6
h	14

From fig 4.2, it can be deduced that the planar antenna operates in 865 MHz band with bandwidth of 238.6 MHz (25.08%). Since the planar design confirms that this antenna has wideband capability, it is then modified to conformal structure without any changes.

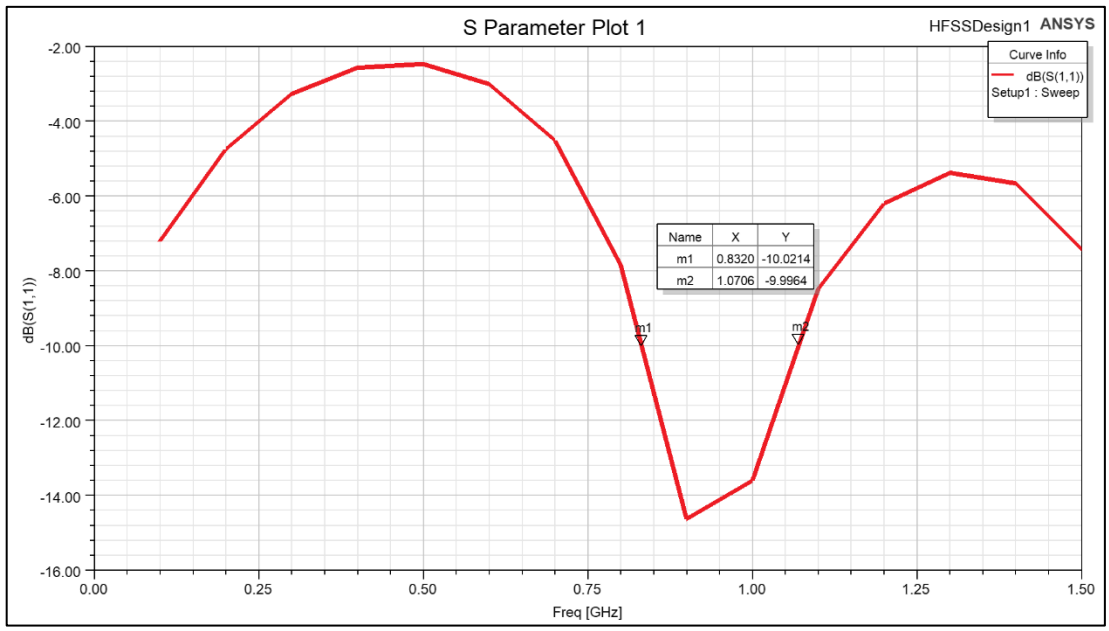

Figure 4.2 Return loss vs Frequency

4.1.2 Conformal design

The results are obtained from the simulation software. From fig. 4.4, it is observed that the designed antenna operates from 833.5 MHz to 1110.7 MHz (28.51

%). The maximal realized gain of the antenna is found to be -18.1 dBi and the SAR value is 1.5933 W/kg when incident power is 2.7 mW at 865 MHz (see fig. 4.5 and fig. 4.8). 2D Radiation patterns are also observed in fig. 4.6 and fig. 4.7.

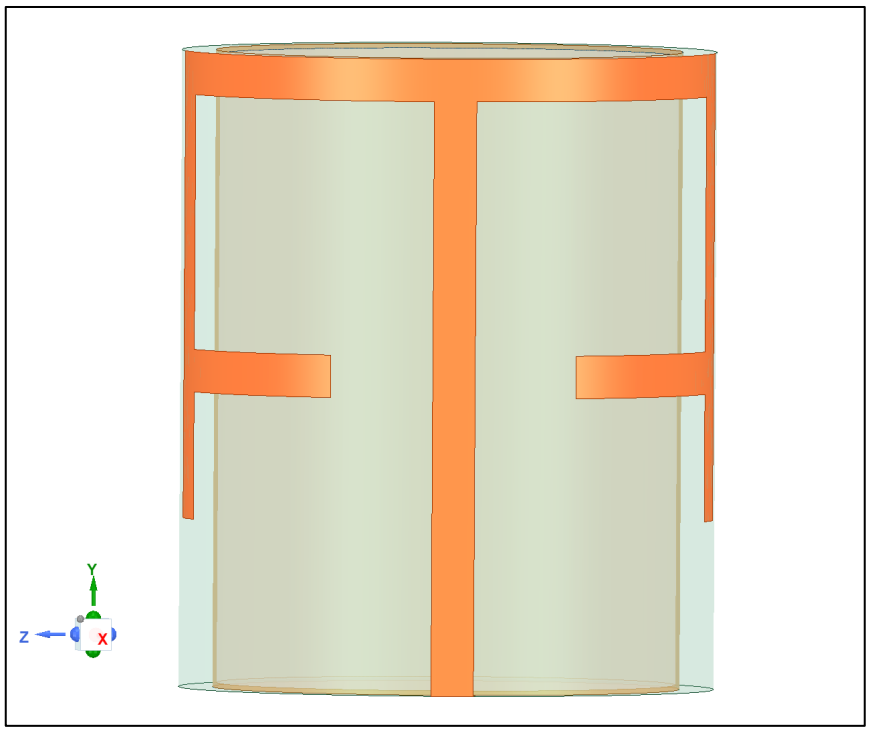

Figure 4.3 Conformal design of antenna

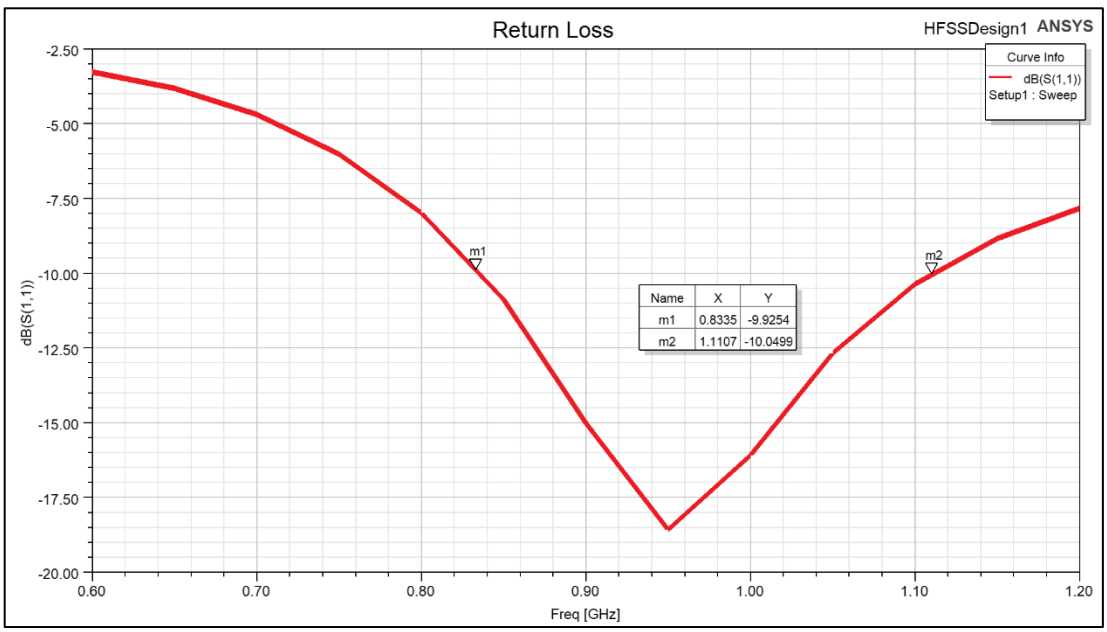

Figure 4.4 Return loss vs Frequency

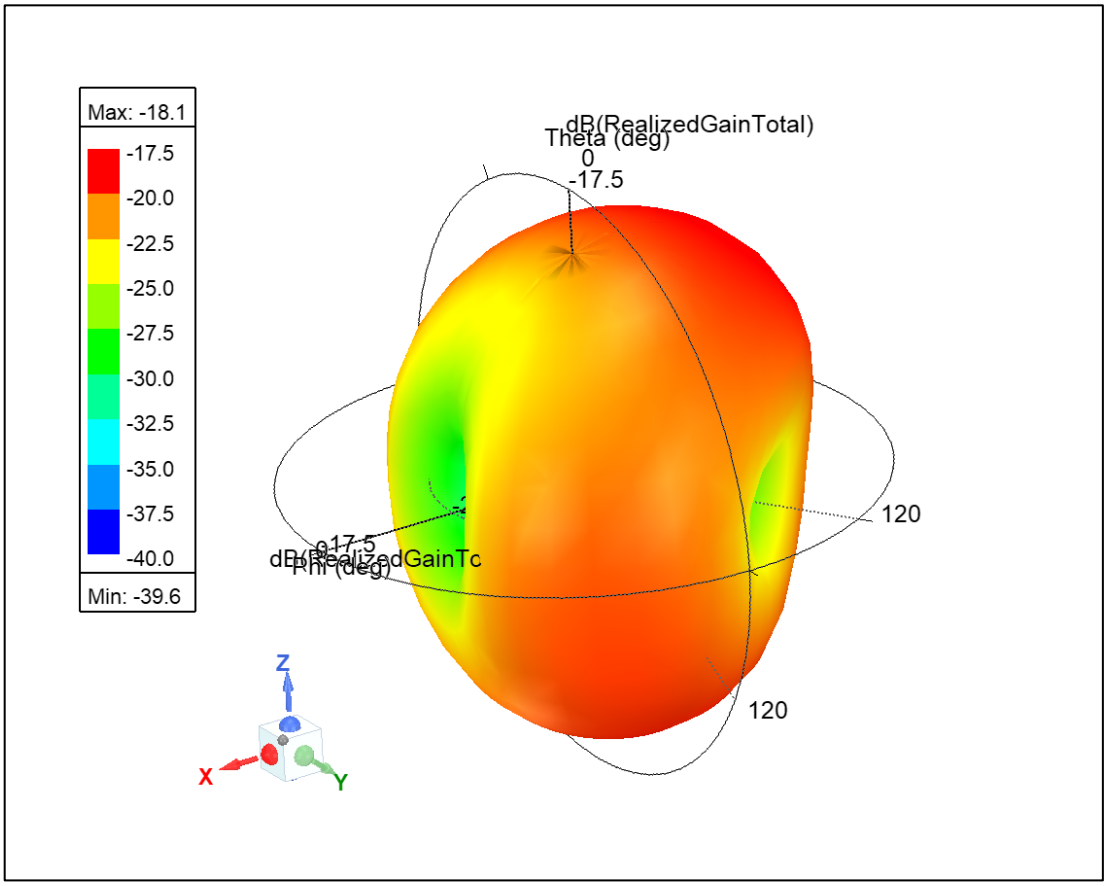

Figure 4.5 3D Radiation pattern

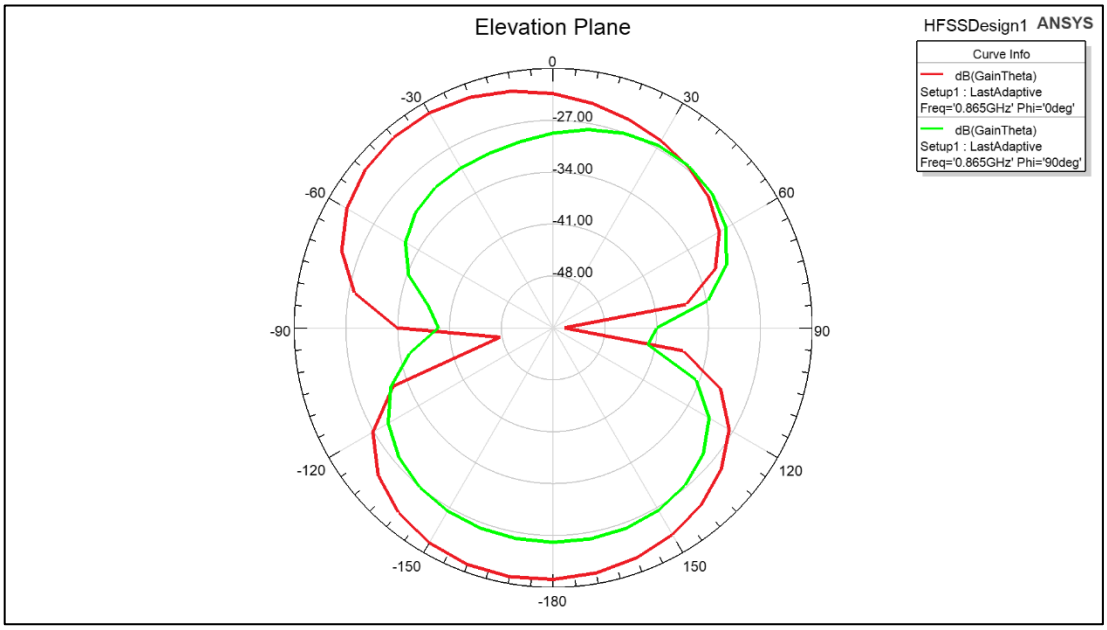

Figure 4.6 Elevation Plane

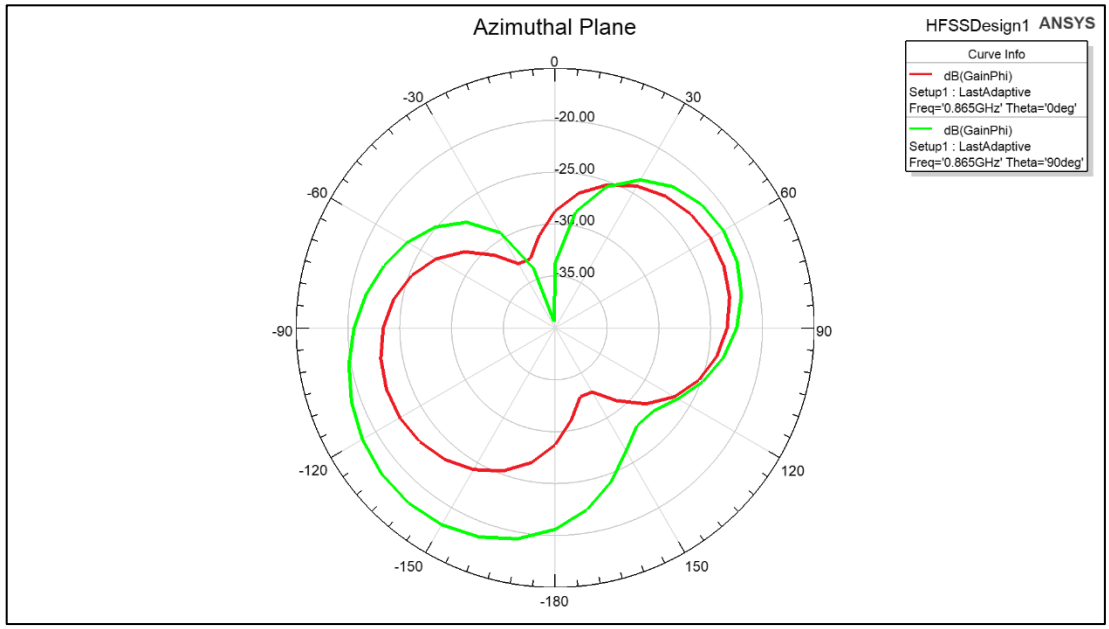

Figure 4.7 Azimuthal Plane

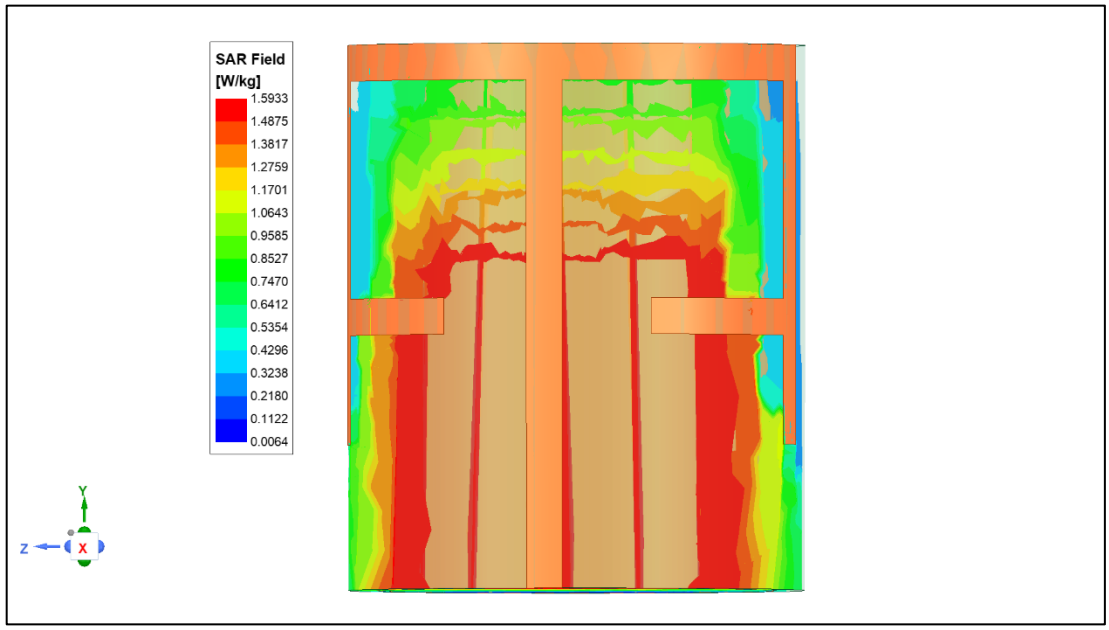

Figure 4.8 SAR field

4.2 ANTENNA-2

Here the structure of the radiator is modified and is made into bow and arrow shape as illustrated in fig. 4.9. Similarly, the antenna is conformed around the exterior of the capsule (see fig. 4. 11). The parametric measurements of the antenna are discussed in Table III.

4.2.1 Planar design

From fig 4.10, it can be deduced that the antenna operates in both 865 MHz band and 2.4 GHz band. At 865 MHz, bandwidth is 224.5 MHz (22.5%) and operates beyond 2.0443 GHz depicting antenna's wideband nature at 2.4 GHz. Since the planar design confirms that this antenna has wideband and multiband capability, it is further modified to conformal structure without any changes.

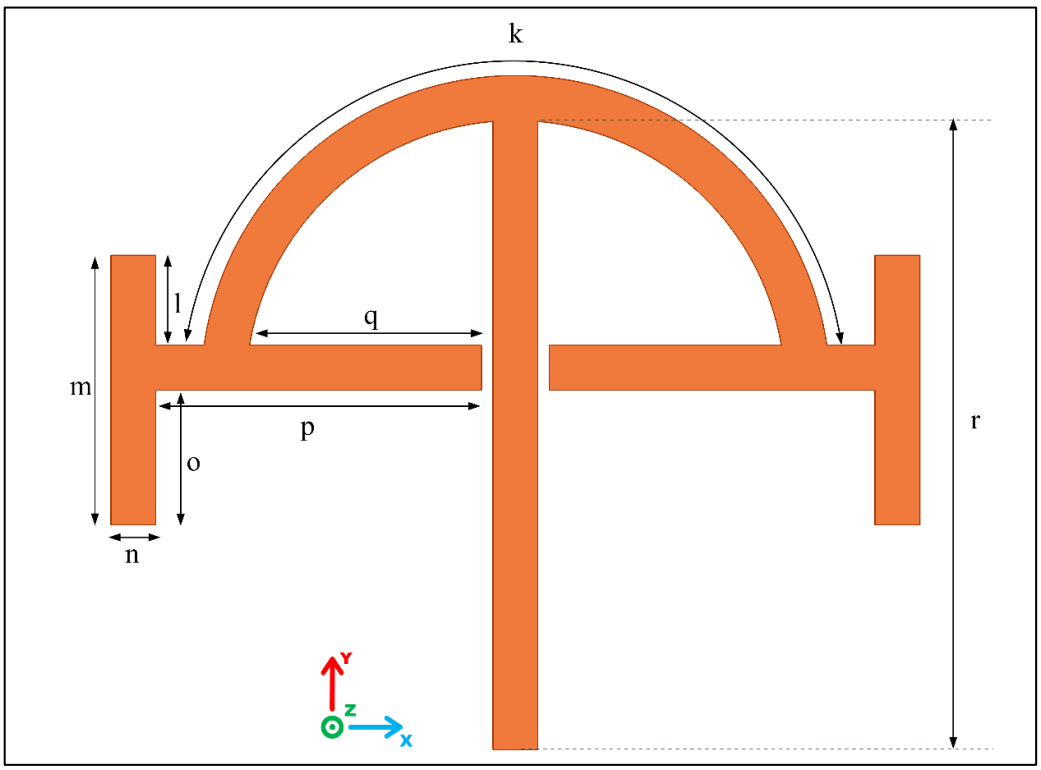

Figure 4.9 Planar design of antenna

Table III. Dimensions of antenna

DIMENSIONS	VALUE (mm)
k	19.98
l	2
m	6
n	1
o	3
p	7.25
q	5.17
r	13.98

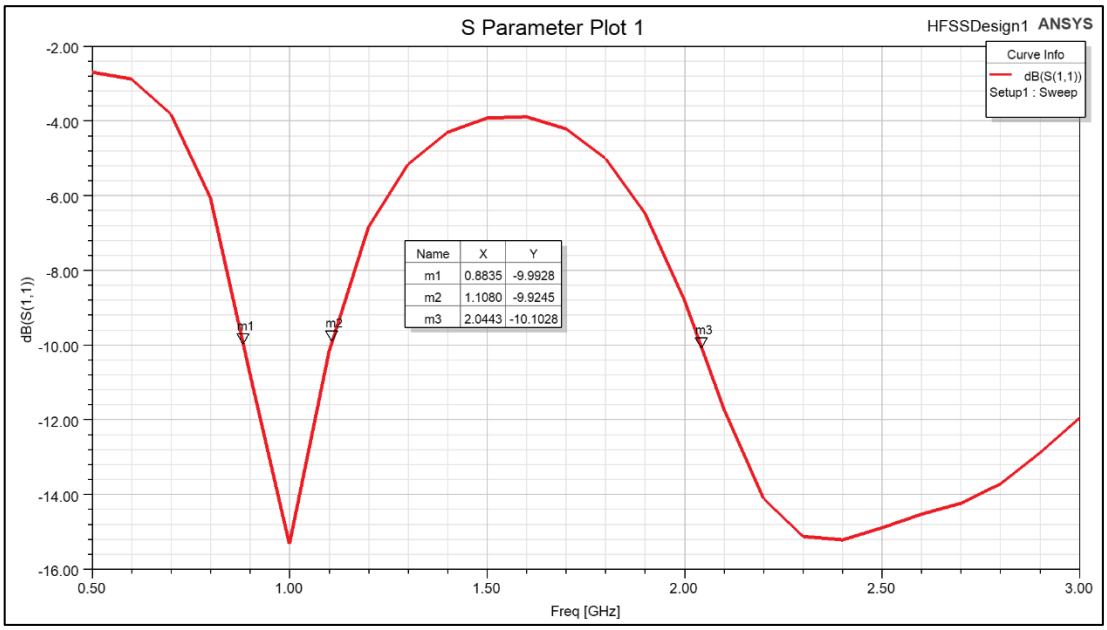

Figure 4.10 Return loss vs Frequency

4.2.2 Conformal design

The results are obtained from the simulation software. From fig. 4.12, it is observed that the antenna operates from 858.2 MHz to 1132.1 MHz (27.52 %) and beyond 2.1648 GHz (wideband). The gain of the antenna is found out to be -18.1 dBi and the SAR value is 1.5859 W/kg when incident power is 2.5 mW at 865 MHz (see fig. 4.13 and fig. 4.16) while at 2.4 GHz, peak gain of the antenna is found out to be -13.3 dBi and the SAR value is 1.5859 W/kg when power supply is 7.4 mW (see fig. 4.17 and fig. 4.20). 2D Radiation patterns at 865 MHz and 2.4 GHz are observed in fig. 4.14 & fig. 4.15 and 4.18 & fig. 4.19, respectively.

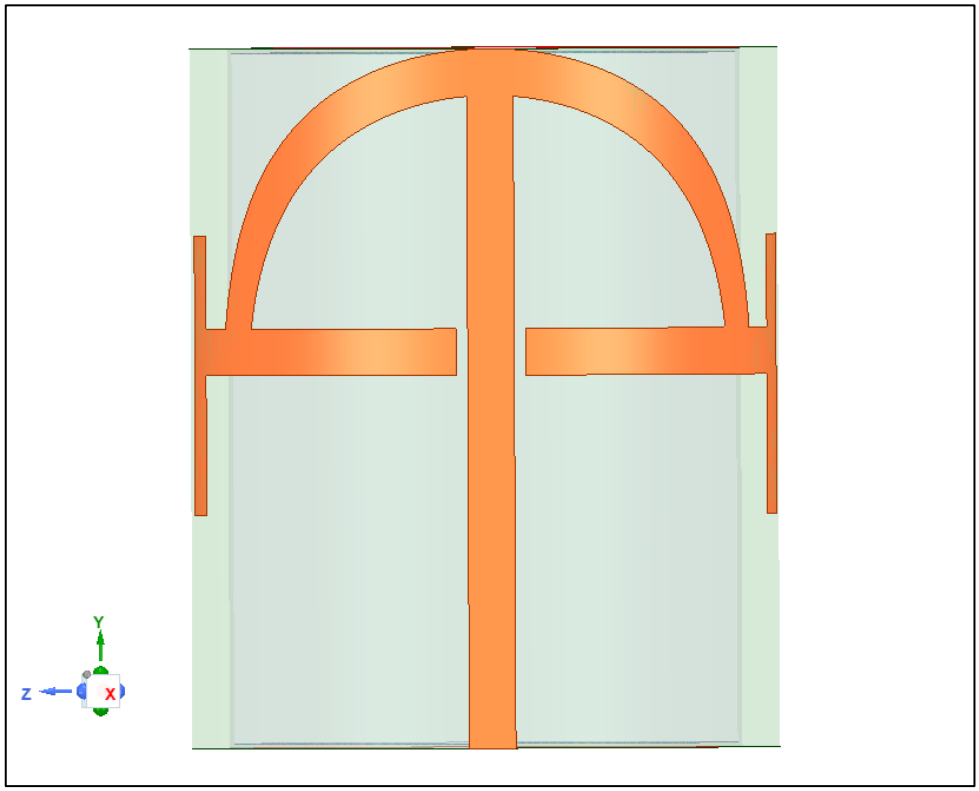

Figure 4.11 Conformal design of antenna

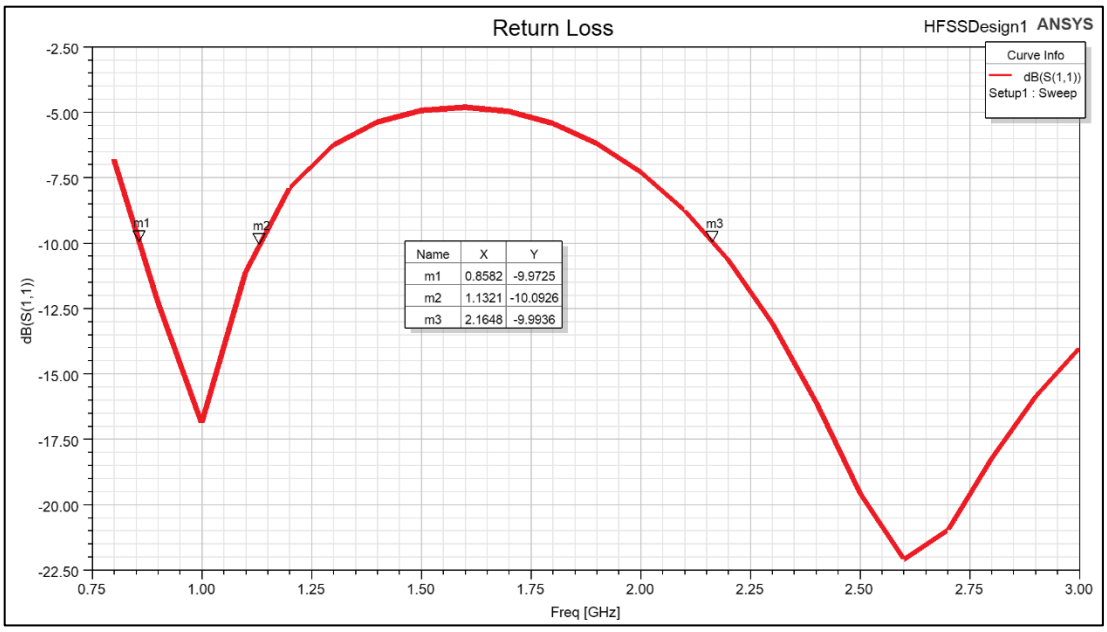

Figure 4.12 Return loss vs Frequency

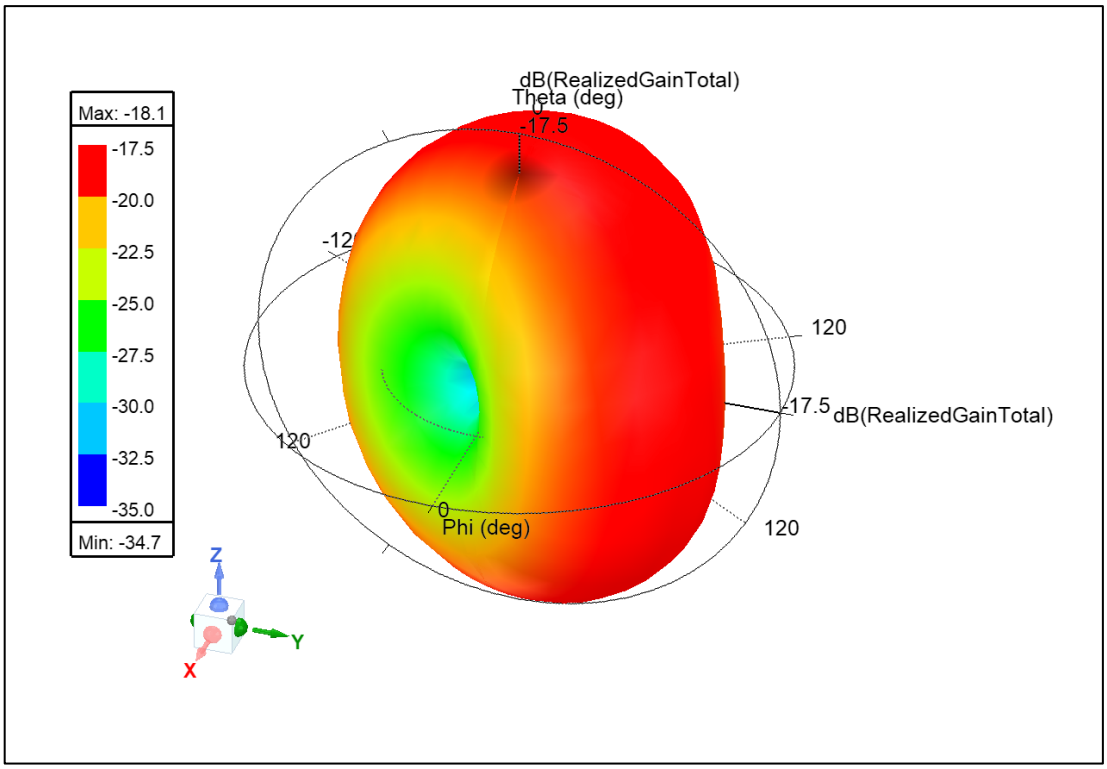

Figure 4.13 3D Radiation pattern

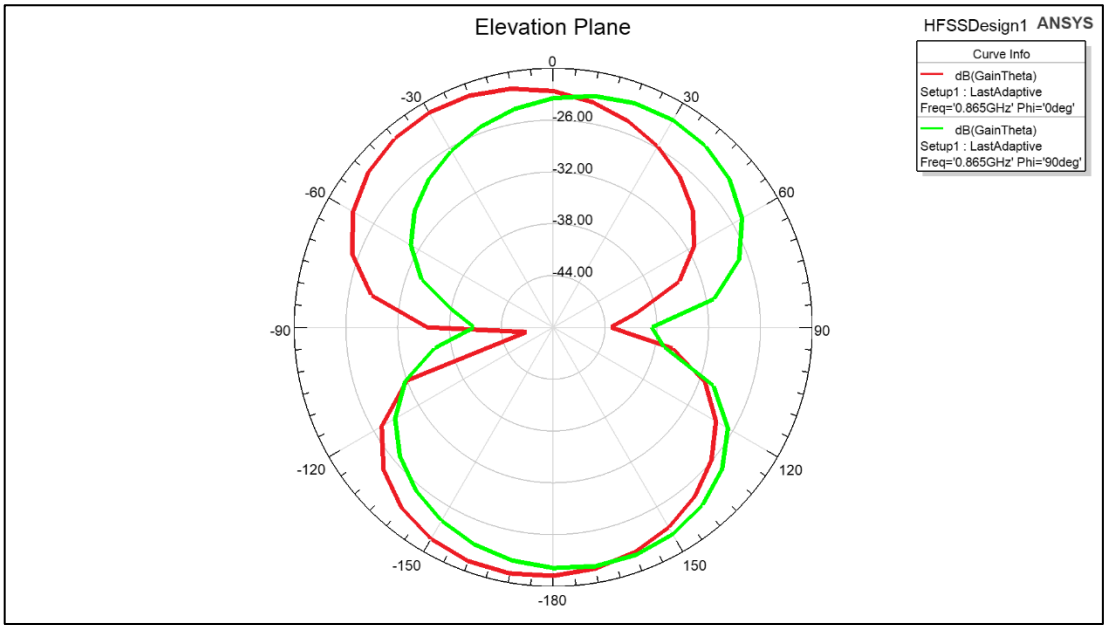

Figure 4.14 Elevation Plane

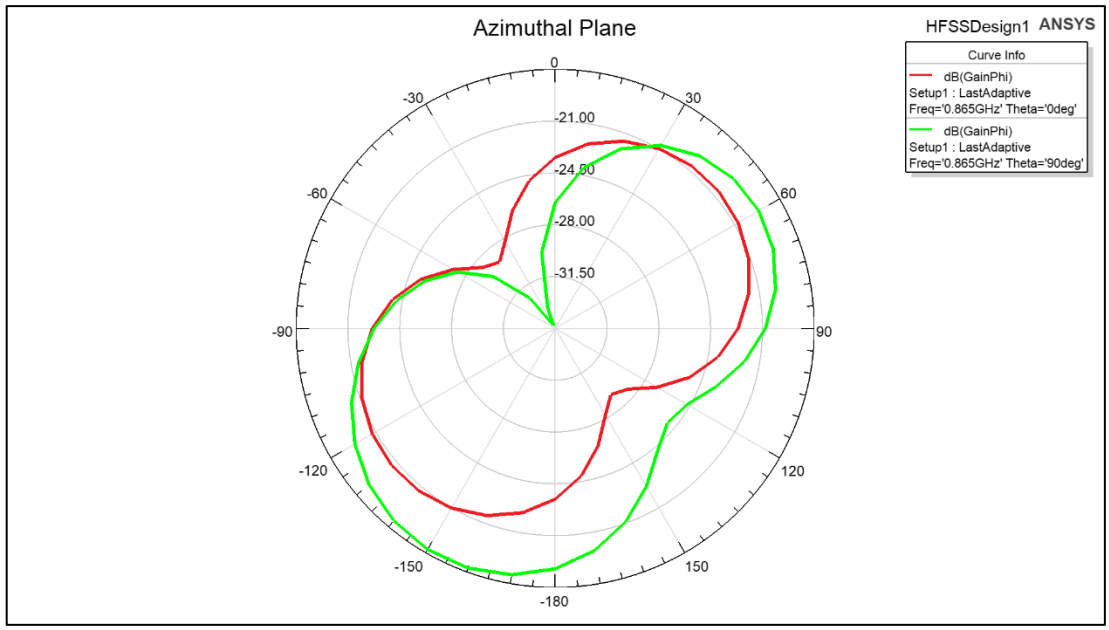

Figure 4.15 Azimuthal Plane

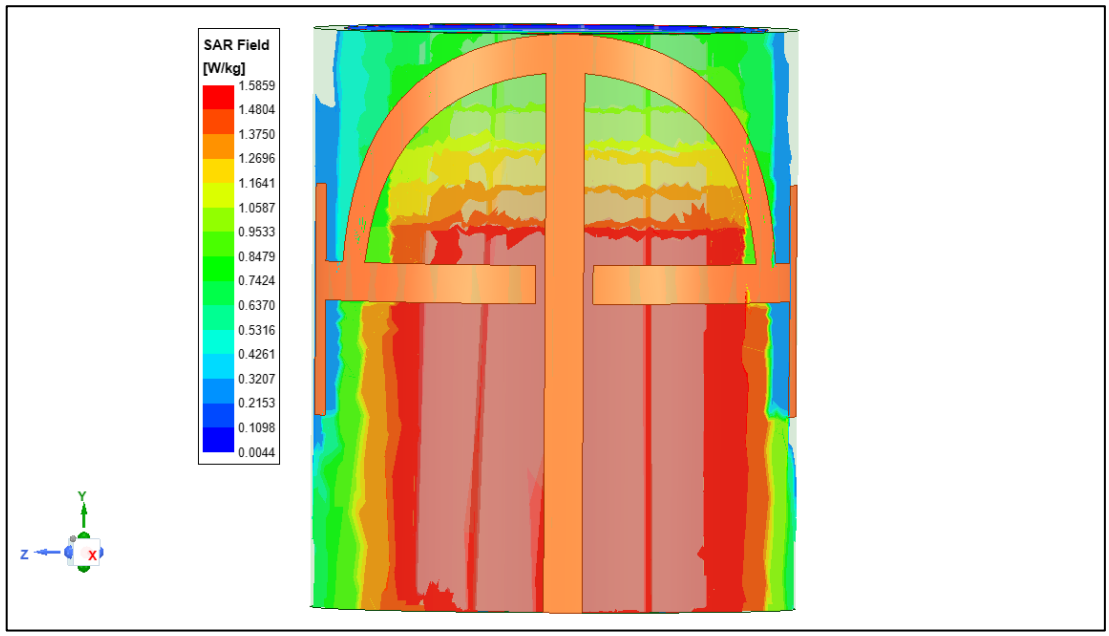

Figure 4.16 SAR field

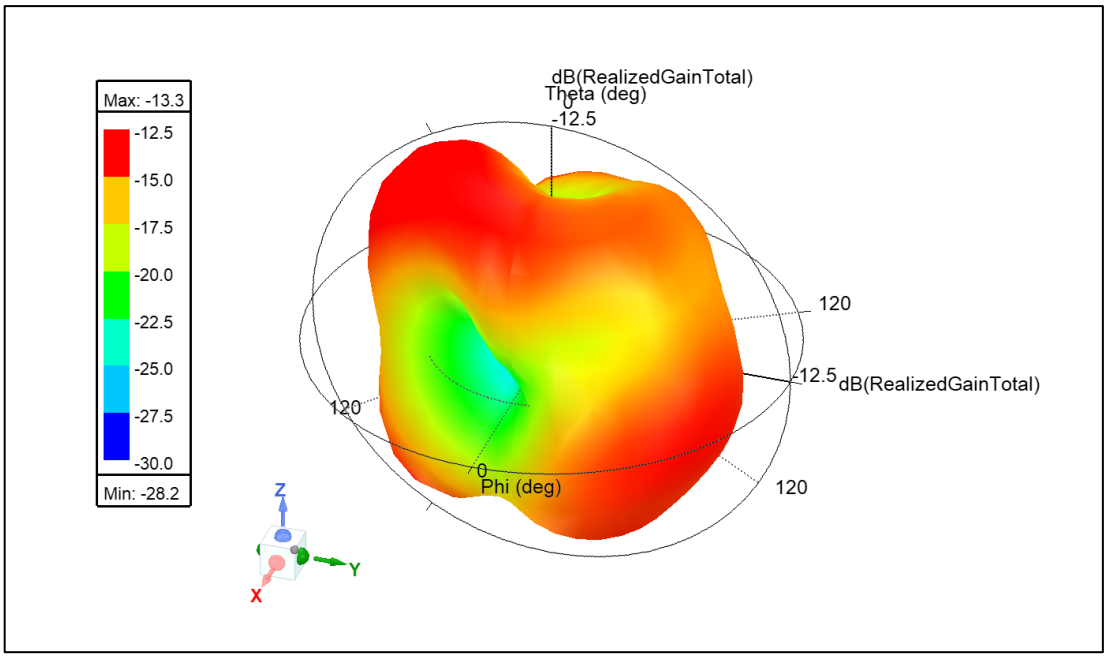

Figure 4.17 3D Radiation pattern

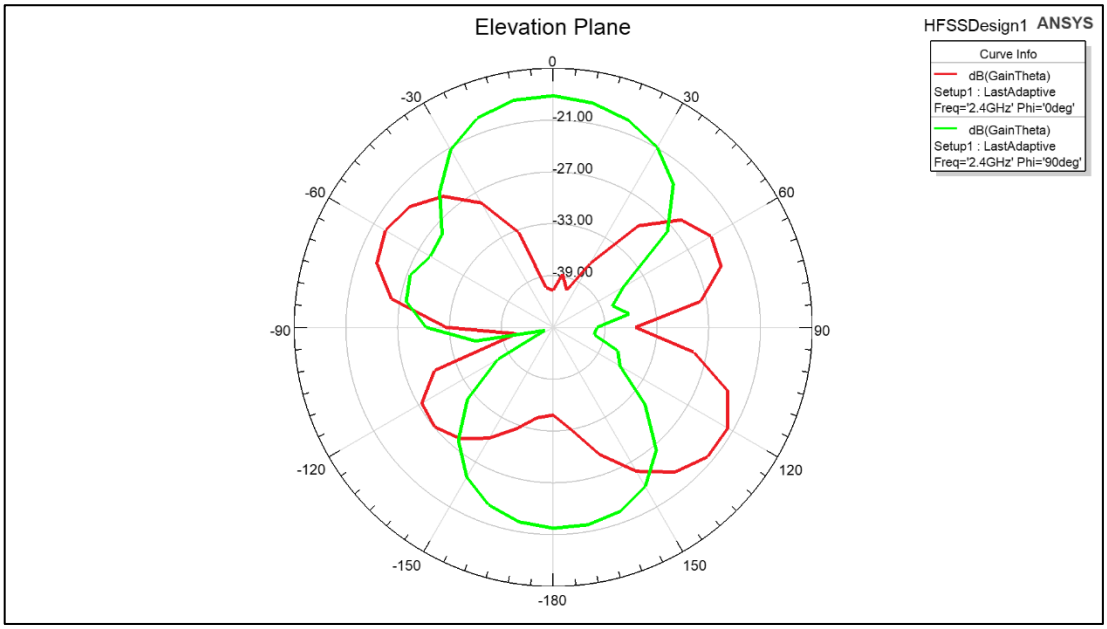

Figure 4.18 Elevation Plane

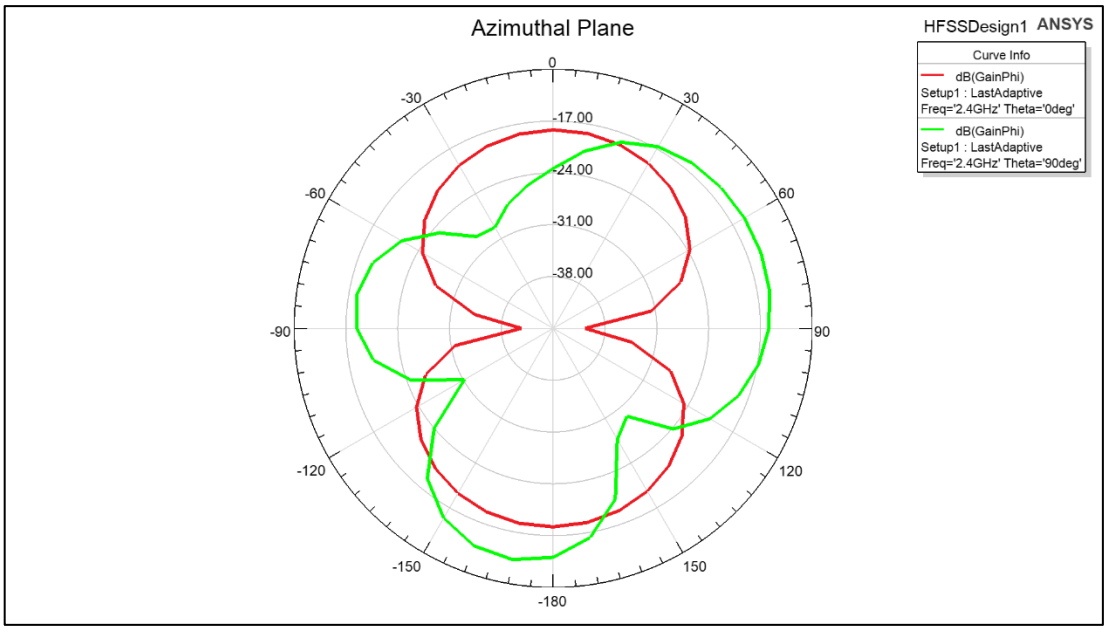

Figure 4.19 Azimuthal Plane

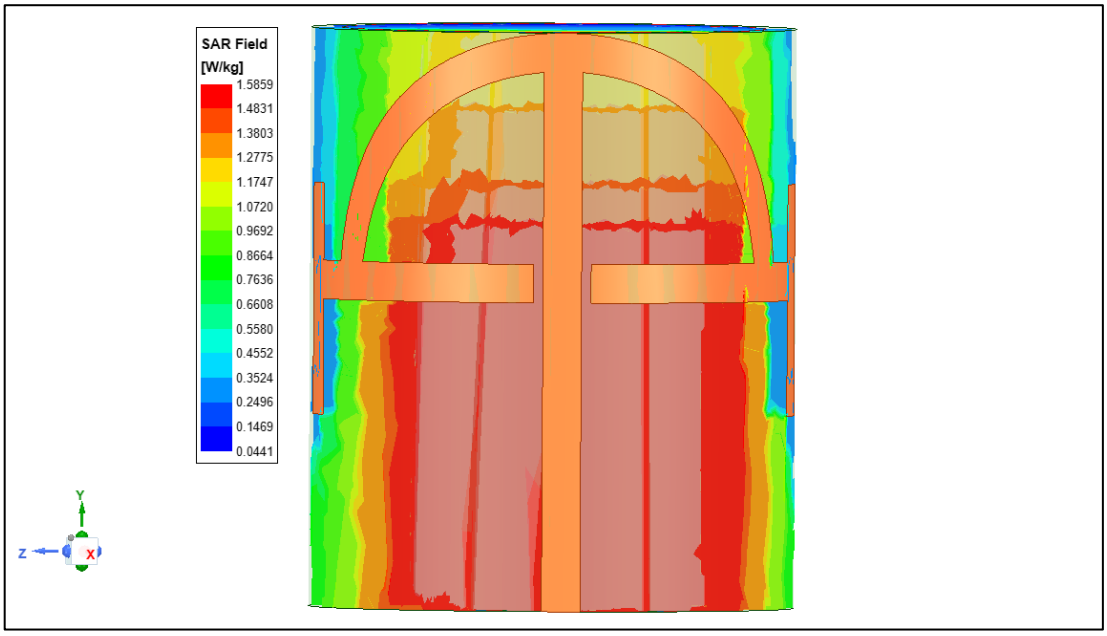

Figure 4.20 SAR field

4.3 CHANGING BATTERY LENGTH

Since batteries are larger components inside the capsule, their impact on bandwidth needs to be explored. The length of the battery was modified to 0 mm, 5 mm, and 10

mm in three instances (see fig. 4.21). It is observed that varying the lengths of battery does not affect the bandwidth (see fig. 4.22).

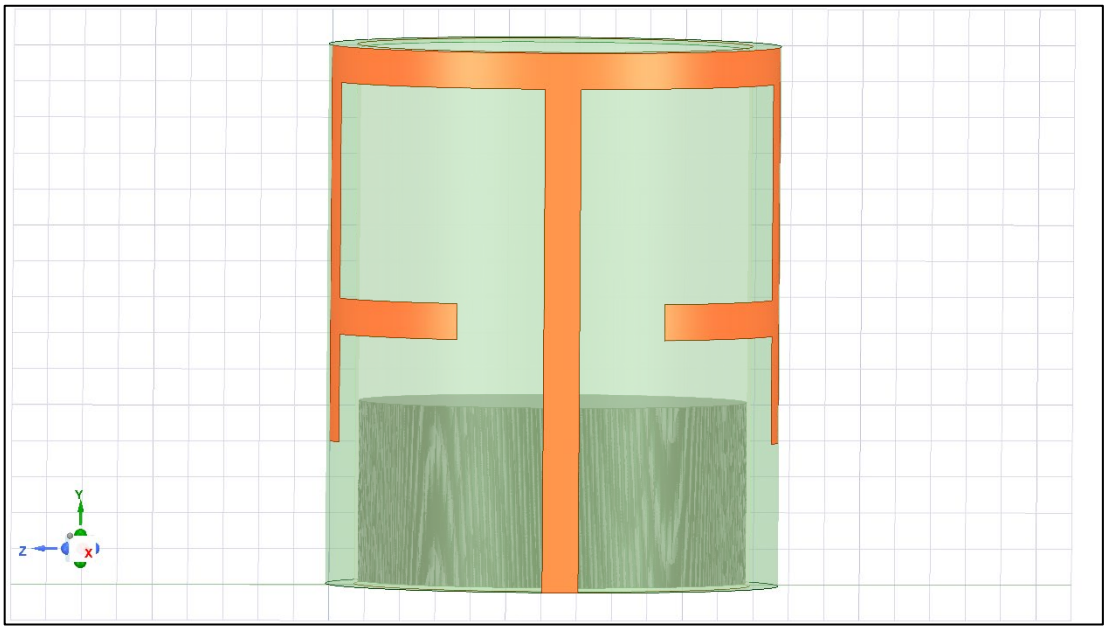

Figure 4.21 Simulation design

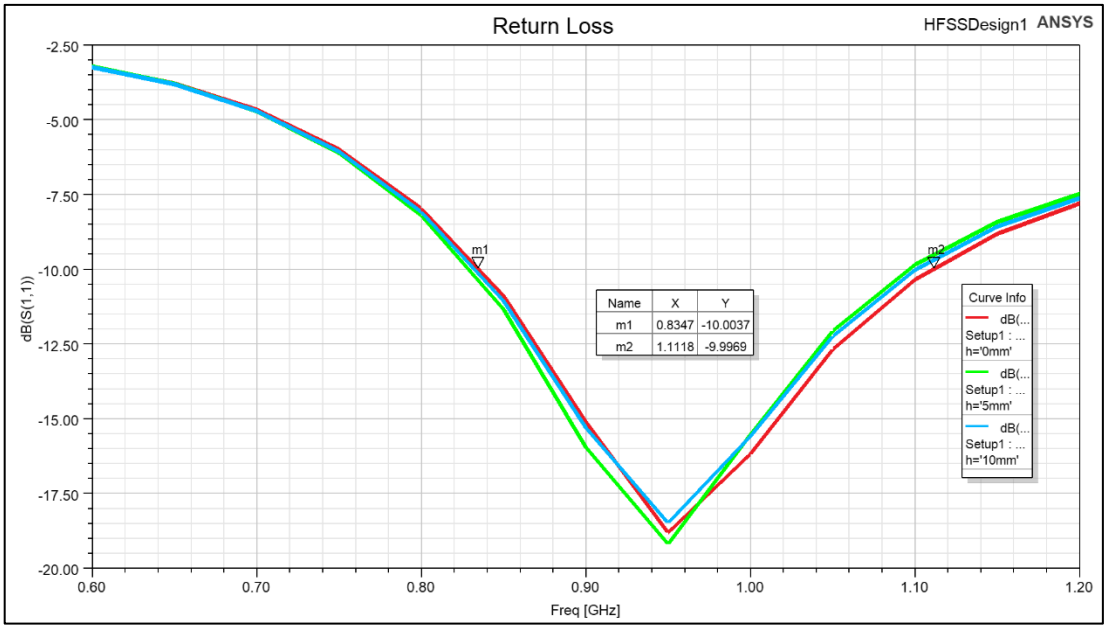

Figure 4.22 Return loss vs Frequency

CHAPTER 5

CONCLUSION AND FUTURE SCOPE

A single layer, wideband, compact, and low SAR implantable antenna for biotelemetry applications. The antenna comprises a rectangular C-shaped radiator and an inverted rectangular C-shaped ground plane. The antenna works at MedRadio, WMTS band, and ISM (433 MHz, 865 MHz, and 2.4 GHz) bands with wider bandwidth. A maximum gain of -14.6 dBi is obtained with a peak SAR of 1.5997 W/Kg with an incident power of 9.85 mW. By changing two parameters namely 'a' and 't', the effect of parametric change on the antenna has been studied. Further, polyamide (ε_r = 4.3) and alumina ceramic (ε_r = 9.8) pair are used as substrate and superstrate respectively, for biocompatibility purposes, without altering the structure of this antenna. Peak SAR value of 1.5915 W/Kg is observed at an incident power of 23 mW and peak gain of -6.3 dBi is observed.

For wireless capsule endoscopy, two conformal wideband antennas are designed. Both the antennas operate in the 865 MHz band while one of them also operates in 2.4 GHz band. First two planar antennas are designed, then they are conformed around a cylindrical capsule. The simulation is performed in AEDT simulation software, and it is observed that the antennas have wider bandwidth at respective bands. The peak realized gain for both antennas at 865 MHz are -18.1 dBi while antenna with bow and arrow shaped radiator has peak realized gain of -13.3 dBi

at 2.4 GHz. At 865 MHz with power input < 2.5 mW and at 2.4 GHz with power input < 7.4 mW, satisfactory SAR values are obtained for bow and arrow shaped radiator. Biocompatibility has been ensured in the antennas discussed in this report.

In this project, a multilayer model (muscle, bones, and fat layer) has not been used, so this model can be considered in the future to get more precise and error-free results. Also, the gain must be improved even though the size of the antenna is very small in comparison to the wavelength. Further, the antenna can be fabricated and tested, and the results can be compared with the simulation results.

REFERENCES

[1] Capsule Endoscopy: Preparation, Pros, Cons | Lubbock Gastro", *Lubbock Gastroenterology*, 2022. [Online]. Available: https://lubbockgastro.com/services/capsule-endoscopy/

[2] C. Wu, T. Chien, C. Yang and C. Luo, "Design of Novel S-Shaped Quad-Band Antenna for MedRadio/WMTS/ISM Implantable Biotelemetry Applications", *International Journal of Antennas and Propagation*, vol. 2012, pp. 1-12, 2012.

[3] A. Kiourti and K. Nikita, "Implantable Antennas", *IEEE Microwave Magazine*, no. 4, pp. 77-91, 2014.

[4] B. Biswas, A. Karmakar and V. Chandra, "Miniaturised wideband ingestible antenna for wireless capsule endoscopy", *IET Microwaves, Antennas & Propagation*, vol. 14, no. 4, pp. 293-301, 2020.

[5] Z. Xia et al., "A Wideband Circularly Polarized Implantable Patch Antenna for ISM Band Biomedical Applications", *IEEE Transactions on Antennas and Propagation*, vol. 68, no. 3, pp. 2399-2404, 2020.

[6] M. Singh, J. Ghosh, S. Ghosh and A. Sarkhel, "Miniaturized Dual-Antenna System for Implantable Biotelemetry Application", IEEE Antennas and Wireless Propagation Letters, vol. 20, no. 8, pp. 1394-1398, 2021.

[7] C. Liu, Y. Guo and S. Xiao, "Compact Dual-Band Antenna for Implantable Devices", *IEEE Antennas and Wireless Propagation Letters*, vol. 11, pp. 1508-1511, 2012.

[8] C. Tsai, K. Chen and C. Yang, "Implantable Wideband Low-SAR Antenna With C-Shaped Coupled Ground", *IEEE Antennas and Wireless Propagation Letters*, vol. 14, pp. 1594-1597, 2015.

[9] J. Faerber, G. Cummins and M. Desmulliez, "Design of conformal wideband antennas for capsule endoscopy within a body tissue environment", *2016 46th European Microwave Conference (EuMC)*, 2016.

[10] S. Kim and H. Shin, "An Ultra-Wideband Conformal Meandered Loop Antenna for Wireless Capsule Endoscopy", *Journal of Electromagnetic Engineering and Science*, vol. 19, no. 2, pp. 101-106, 2019.

[11] M. S. Miah, A. N. Khan, C. Icheln, K. Haneda, and K. I.Takizawa, "Antenna systems for wireless capsule endoscope: Design, analysis and experimental validation," *IEEE Transactions on Antennas and Propagation*, pp. 1–11, 2018.

[12] S. Yun, K. Kim and S. Nam, "Outer-Wall Loop Antenna for Ultrawideband Capsule Endoscope System", *IEEE Antennas and Wireless Propagation Letters,* vol. 9, pp. 1135-1138, 2010.

[13] J. Wang, M. Leach, E. Lim, Z. Wang, R. Pei and Y. Huang, "An Implantable and Conformal Antenna for Wireless Capsule Endoscopy", *IEEE Antennas and Wireless Propagation Letters*, vol. 17, no. 7, pp. 1153-1157, 2018.

[14] N. Malik, P. Sant, T. Ajmal and M. Ur-Rehman, "Implantable Antennas for Bio-Medical Applications", *IEEE Journal of Electromagnetics, RF and Microwaves in Medicine and Biology*, vol. 5, no. 1, pp. 84-96, 2021.

[15] S. Lee et al., "A Wideband Spiral Antenna for Ingestible Capsule Endoscope Systems: Experimental Results in a Human Phantom and a Pig", *IEEE Transactions on Biomedical Engineering*, vol. 58, no. 6, pp. 1734-1741, 2011.

[16] C.A. Balanis, *Antenna Theory: Analysis and Design*, John Wiley and Sons, 1982.